THE GAMMA-RADIATION PATTERN OF A CYLINDRICAL WATER-MODERATED SUBCRITICAL ASSEMBLY

by

Frederick Francis Gerschboth

A Thesis Submitted to the
Graduate Faculty in Partial Fulfillment of
The Requirements for the Degree of
MASTER OF SCIENCE

Major Subject: Engineering

Iowa State College
1957

TABLE OF CONTENTS

TABLE OF CONTENTS (Continued)

I. SUMMARY

On the occasion of a conference of the American Society for Engineering Education held in June of 1956 at Iowa State College, a modified copy of a subcritical assembly designed by the members of the Physics staff of the New York University was made available by the Atomic Energy Commission. After the assembly of this device was completed at the location for display, routine radiation monitoring was conducted. Rather than the expected symmetrical radiation pattern, definite "hot spots" of gamma radiation were noted at various locations around the circumference of the cylindrical wall. Further, at the location of these unusually high gamma counts inordinately low neutron counts were measured.

The problem was brought to the attention of the author that an analysis might be effected to perhaps provide helpful data in any projected design of similar assemblies.

Upon examination of the physical arrangement of the lattice of the assembly, it was intuitively postulated that these hot spots resulted from discontinuities in the hexagonal uranium lattice, since they coincided with the vertices of the lattice. The height of these hot spots coincided with the horizontal plane that encompassed the center of the radium-berillyium source in the assembly.

Thus, it was thought that the unduly high gamma radiation was caused by the lack of gamma absorption resulting from the

paucity of uranium across the lines running from the center to the vertices of the lattice; as, on the other hand, in these same regions, the lack of fuel for neutron multiplication explained the low neutron count. In effect, at the vertices of the lattice, there were free paths from the source through the moderator to the counter. Moreover, the radiation pattern was further modified by the effects of the gamma scattering, multiplication and absorption in the lattice.

This thesis is concerned with the pattern of the gamma radiation of the assembly described.

II. INTRODUCTION

A. Statement of Problem

The problem consisted of a measurement and analysis of the gamma-radiation pattern resulting from a radium-beryllium point source suspended in a cylindrical assembly consisting of a water moderator and a symmetrical hexagonal lattice of natural uranium.

B. Scope of the Problem

The scope of this thesis was limited to the gamma radiation pattern pattern. The analysis was made only in the horizontal plane of the source to limit repeated calculations. For the same reason the analysis was confined to one sextant of the lattice -- a simplification considered justifiable in view of the symmetry of the lattice.

III. INVESTIGATION

A. Objectives

The primary objectives of this investigation were the providing of a theoretical analysis (and measurements for comparison) of the assembly under discussion. The secondary objectives embraced the developing of a simplified method of analysis for gamma diffusion as well as providing data for use in design problems of similar assemblies.

B. Assumptions

The general assumptions employed in the theoretical analysis of the radiation pattern included the following:

1. Scattering in a homogeneous medium was assumed to be reciprocal. Thus, the radiation scattered from a path traversing an area in a homogeneous medium (e.g. the water outside the lattice) equalled the radiation scattered into that path from adjacent paths through the water.

2. The radium-beryllium source used with the assembly under study was assumed to be a point source.

Specific assumptions in the course of computations became necessary and are noted as they occur.

IV. THEORETICAL ANALYSIS

A. Diffusion of Gamma-Rays from External Source

1. Source components

The source used with this assembly was a 100 millicurie radium-beryllium source. The products of the radium disintegration are as follows: (5, p. 11 and 15, pp. 5-90)

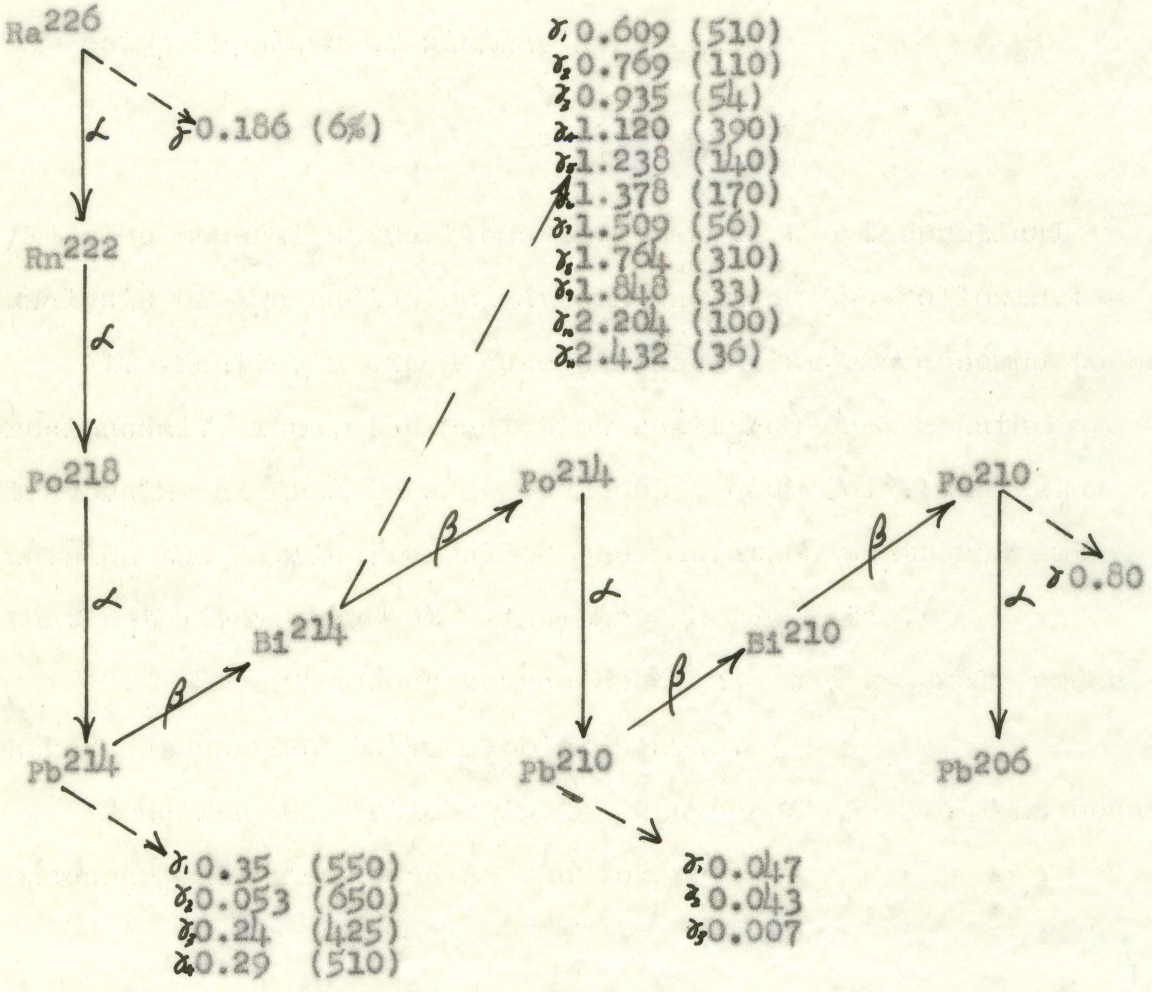

In depicting the radium decay scheme the principal branch of each branching decay was utilized. Since the major branch-

ings are favored to the extent of 99.98 per cent versus 0.02 per cent, this simplification is justifiable. The gamma-rays included in the diagram then are expected as a result of the radium decay in the extraneous source.

Because there are alternate methods of effecting the gamma-transitions, not all of the above-listed gamma-rays will be produced in every disintegration of the radium. In addition, some of the gamma-rays are of such low energy that their absorption along the source-to-detector-path is assured. Thus they may be eliminated from the calculations. Finally, because of the twenty-two year half-life of Pb^{210}, few of the gamma-rays resulting from transitions occurring past Pb^{210} in the decay pattern can be expected.

For reason of low energy then, the 0.186, 0.047, 0.05, 0.043, and 0.007 Mev gamma-rays can be eliminated. Because of the long half-life of Pb^{210}, the 0.80 Mev gamma-ray can be ignored. In the decay of Pb^{214} there are four means by which the transformation to the ground state can be made. These transformations consist of a combination of a β emission and one of the following gamma-radiations: 0.35, 0.053, 0.24, or 0.29 Mev. Since the 0.05 Mev gamma-ray has already been eliminated, only the 0.35, 0.24, and 0.29 gamma-ray transitions are considered. Since these methods of transition are competitive (as depicted in the Nuclear Science Abstracts, 15, p. 80) one of the three gamma-rays can be expected in each disintegration. Since the energies of all three are so close,

an average energy weighted by the relative frequency of emission of each gamma-ray may be calculated. If the decay scheme in the Nuclear Science Abstracts (15, p. 80) is used, the average energy is found to be 0.3136 Mev. In like manner, the gamma-rays resulting from the decay of Bi^{214} can be divided into three energy groups, and an average energy for each group calculated. The average again is weighted by the relative frequency of emission. Thus, the 0.609, 0.769, and 0.935 Mev gamma-radiations are grouped together, and their average energy is computed to be 0.66 Mev. The second group is composed of the 1.12, 1.238, 1.378, and 1.509 Mev gamma-rays, and their average energy is found to be 1.23 Mev. The last group consists of the 1.764, 1.848, 2.204, and 2.432 Mev gamma-rays, and their average is calculated to be 1.91 Mev. As a result of these simplifications, the source is assumed to be emitting gamma-rays of 0.31, 0.66, 1.23, and 2.432 Mev. In the case of Bi^{214} the contribution of each group will be weighted by the relative frequency of emission of that group. The weightings are 0.353, 0.395 and 0.251 as shown in Appendix B.

2. Source radiation diffusion calculations

a. For paths through the lattice With reference to Figure 2, all paths except those labeled A and B must pass through at least three of the one-inch uranium slugs. If a path composed of three uranium slugs and water is used as a "typical" path through the lattice, absorption calculations

can be made to determine the attenuation caused by lattice absorption. Absorption coefficients to be used in these calculations are provided in Table 1, page 9.

Since the radium-beryllium source used in the experiment was rated at 100 millicuries, 3.7×10^9 disintegrations occur each second. These disintegrations initiate the radium decay chain in which the gamma-rays are born. Since the measurements of the radiation were made on the basis of a square centimeter of area on the outside of the assembly shell, the source strength must be converted into like units. If isotopic scattering from a point source is assumed, the radiation should, at the radius of the shell (24 inches), cover the surface of a spherical shell of that same radius. The area of a sphere of 24 inches radius is determined to be $4.65 \times 10^4 cm^2$. Therefore, at a distance of 24 inches, without absorption, the radiation strength should be

$$\text{Source } (\gamma) = \frac{3.7 \times 10^9}{4.65 \times 10^4}$$

$$S(\gamma) = 7.97 \times 10^5 \text{ photons/cm}^2\text{-sec}$$

This value is equivalent to 4.77×10^6 photons/cm^2-min. The absorption by the uranium in the typical path through the lattice can be calculated from the standard attenuation formula (5, p. 8)

$$R_1 = R_0 e^{-\mu x}$$

Table 1. Gamma absorption coefficients of materials in assembly (13, pp. 17-20)

Energy (Mev)	$\mu(H_2O)^a$ (cm^{-1})	$\mu(H_2O)^b$ (cm^{-1})	$\mu(H_2O)^c$ (cm^{-1})	$\mu(U)^d$ (cm^{-1})	$\mu(U)^e$ (cm^{-1})	$\mu(Fe)^f$ (cm^{-1})	$\mu(Wood)^g$ (cm^{-1})	$\mu(Wood)^h$ (cm^{-1})
0.310	0.13	0.098	0.032	1.57	8.73	2.96	.032	.012
0.660	0.065	0.052	0.033	0.950	1.90	0.21	0.176	.012
0.700	0.063	0.060	0.032	0.770	1.750	0.203	.017	.01
1.000	0.071	0.049	0.032	0.512	1.048	0.195	.015	.0098
1.230	0.065	0.037	0.028	0.438	0.892	0.187	.011	.011
1.910	0.048	0.023	0.025	0.34	0.570	0.156	.006	.010

[a]Linear attenuation coefficient, total, for water

[b]Linear attenuation coefficient of Compton effect for water

[c]Linear attenuation coefficient of absorption for water

[d]Linear attenuation coefficient of Compton effect for uranium

[e]Linear attenuation coefficient of absorption for uranium

[f]Linear attenuation coefficient of absorption for iron

[g]Linear attenuation coefficient of Compton effect for wood

[h]Linear attenuation coefficient of absorption for wood

For 1.91 Mev photons with an absorption coefficient from Table 1 of 0.570 cm^{-1} a value for R_1 of 1.56×10^2 cpm/cm^2 is obtained. This value is further reduced by the absorption of the intervening water in the path. The reduction can again be calculated by the standard attenuation formula with an absorption coefficient for water of 0.025 cm^{-1}. Thus,

$$R_2 = R_1 e^{-\mu x}.$$

R_2 is found to be 87.5 cpm/cm^2. This value is below background (125 cpm) and hence can be ignored. Since the results of these calculations indicate virtually complete absorption of the 1.91 Mev photon in the lattice, it can be deduced that the less energetic photons with the greater absorption coefficients will similarly undergo virtually complete absorption in traversing the lattice. Therefore all gamma-rays under consideration that follow paths C, D, E, F, G, H of Figure 2 will be expected to be absorbed. Because of the symmetry of the lattice this can be generalized to include all paths in the lattice but those at the vertices and those paths adjacent to the vertices (corresponding to paths labeled A and B in Figure 2). Consequently, the radium-beryllium source makes no contribution to the radiation pattern at any point save possibly at the vertices and the nearest points of measurement to the vertices. The paths A and B at the vertices will now be examined.

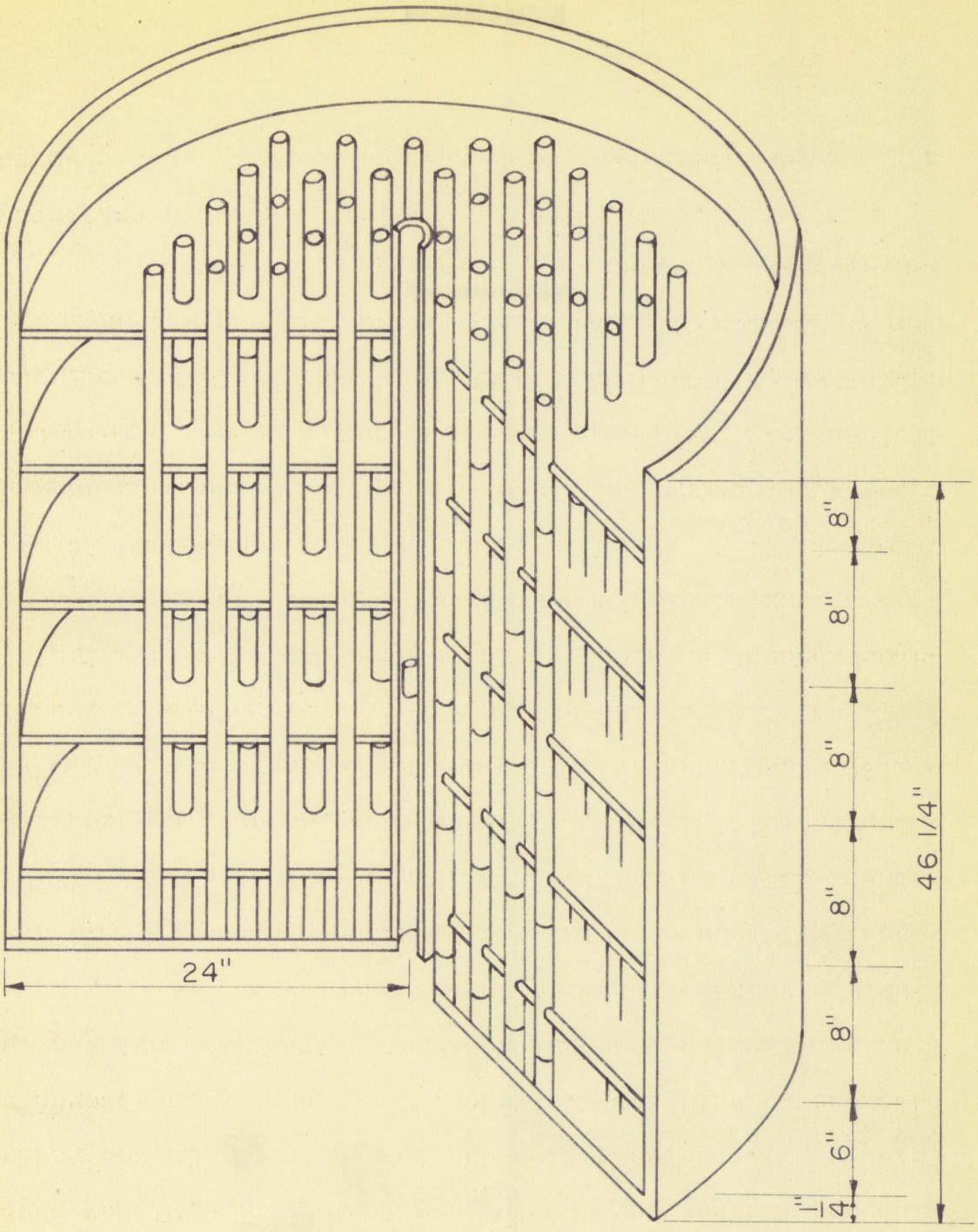

Figure 1. Physical arrangement of assembly

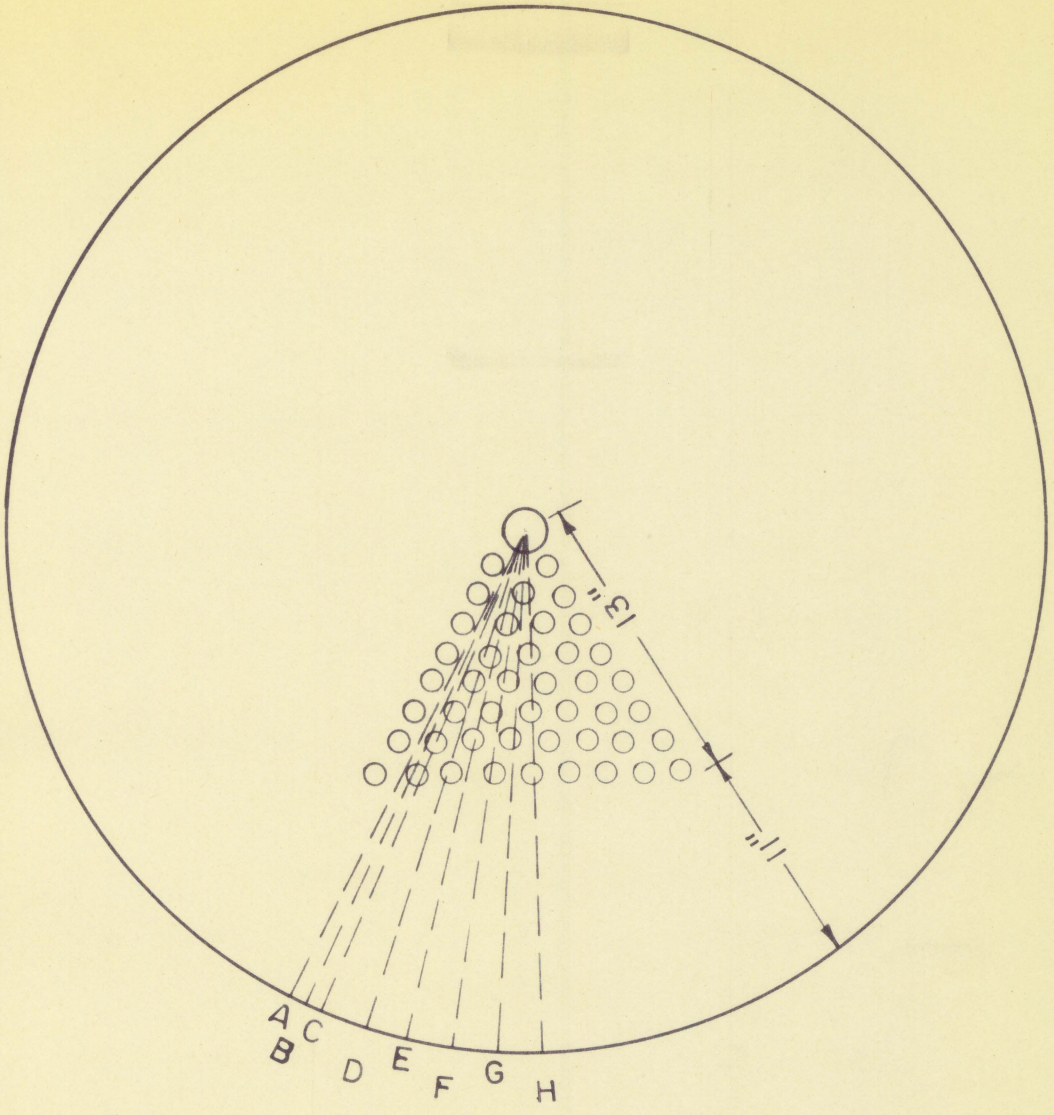

Figure 2. Positions of gamma-radiation measurement

b. At the lattice vertices While scattering was ignored in the preceding calculations (since in all cases the radiation was reduced to values below background by absorption computations alone) because of the lack of the highly-absorbing uranium in the paths at the vertices, consideration must be given to scattering as a means of attenuation in these paths. In anticipation of calculations involving attenuation by scattering the mechanism and effects of this process will be examined.

If photons are scattered out of the low-absorption paths at the vertices into the lattice and absorbed there, the significance of radiation attenuation by scattering is appreciated. However, even in homogeneous media where reciprocal scattering between adjacent paths takes place, the change of direction with its consequent lengthening of path results in a reduction of the radiation level. This effect of scattering upon radiation can be approximated by finding an average angle of scatter, calculating the increase in the length of the radiation path, and finally determining the increased absorption that results from the photons following a longer path in the absorbing medium. To find the average angle of scatter the probability that photons of a specific energy will scatter through specific angles will be used. Latter and Kahn (9) have provided precise values for $\frac{d\sigma}{d\Omega}$, the differential cross section with respect to scattering angle. These probabilities were determined on the basis of the Klein-

Nishina formula for multiple scatterings and have been plotted for various energy photons in Figures 3 through 8. From these plots the average angle of scatter can be calculated.

Let $\sigma = f(\beta)$, the probability density function. Since the total probability must equal unity,

$$\int_0^{180} f(\beta)\, d\beta = 1.$$

If $P(\beta)$ is defined as

$$P(\beta) = C_1 f(\beta)$$

and

$$\int_0^{180} P(\beta)\, d\beta = C_1,$$

the area under the curve $E(\beta)$, the expected value, or the sought average is then found,

$$E(\beta) = \frac{\int_0^{180} \beta\, P(\beta)\, d\beta}{\int_0^{180} 1\, P(\beta)\, d\beta}.$$

By this method, the following values of average scattering angle were calculated for the photon energies of interest.

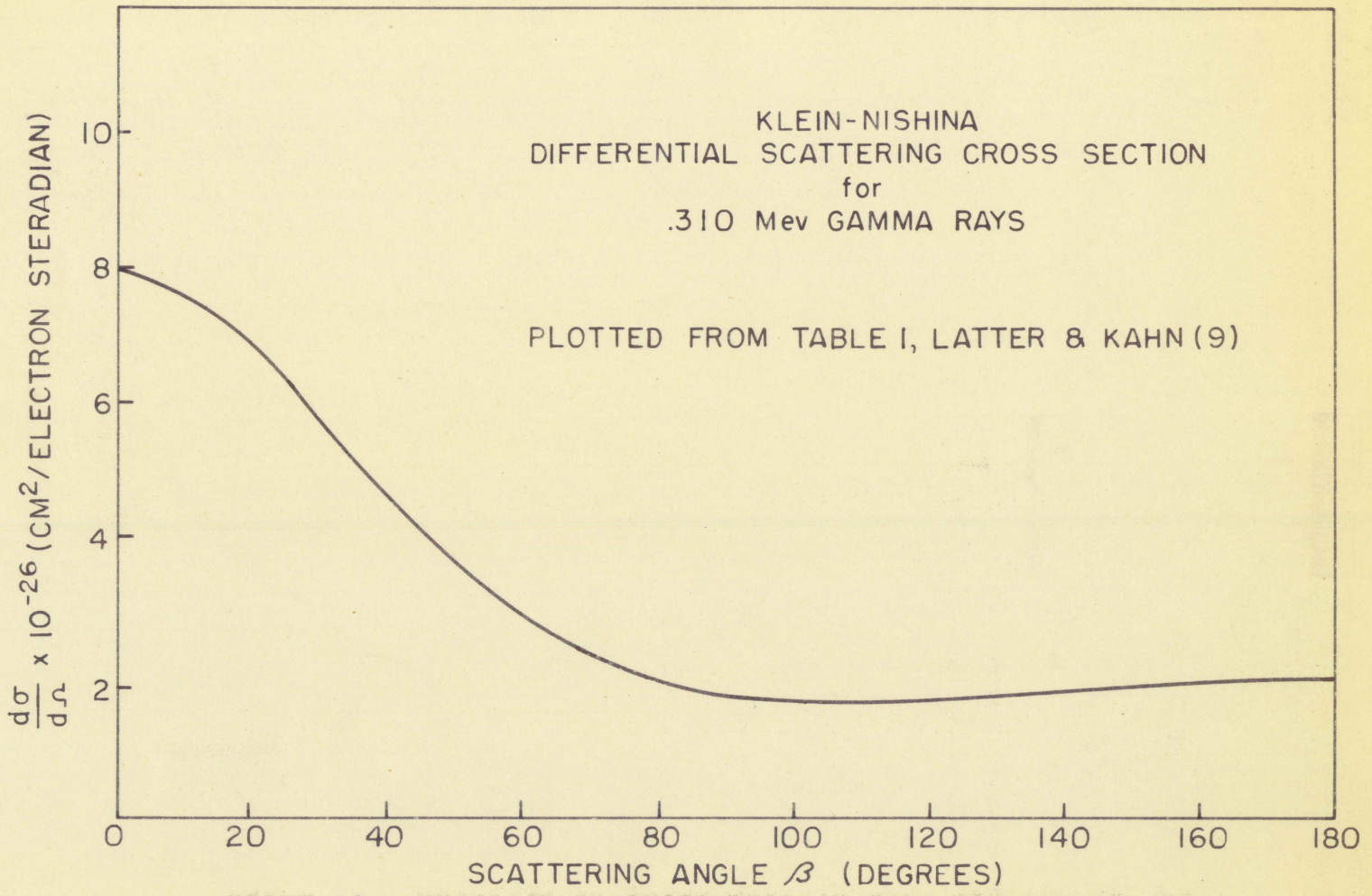

Figure 3. Variation in cross section with scattering angle

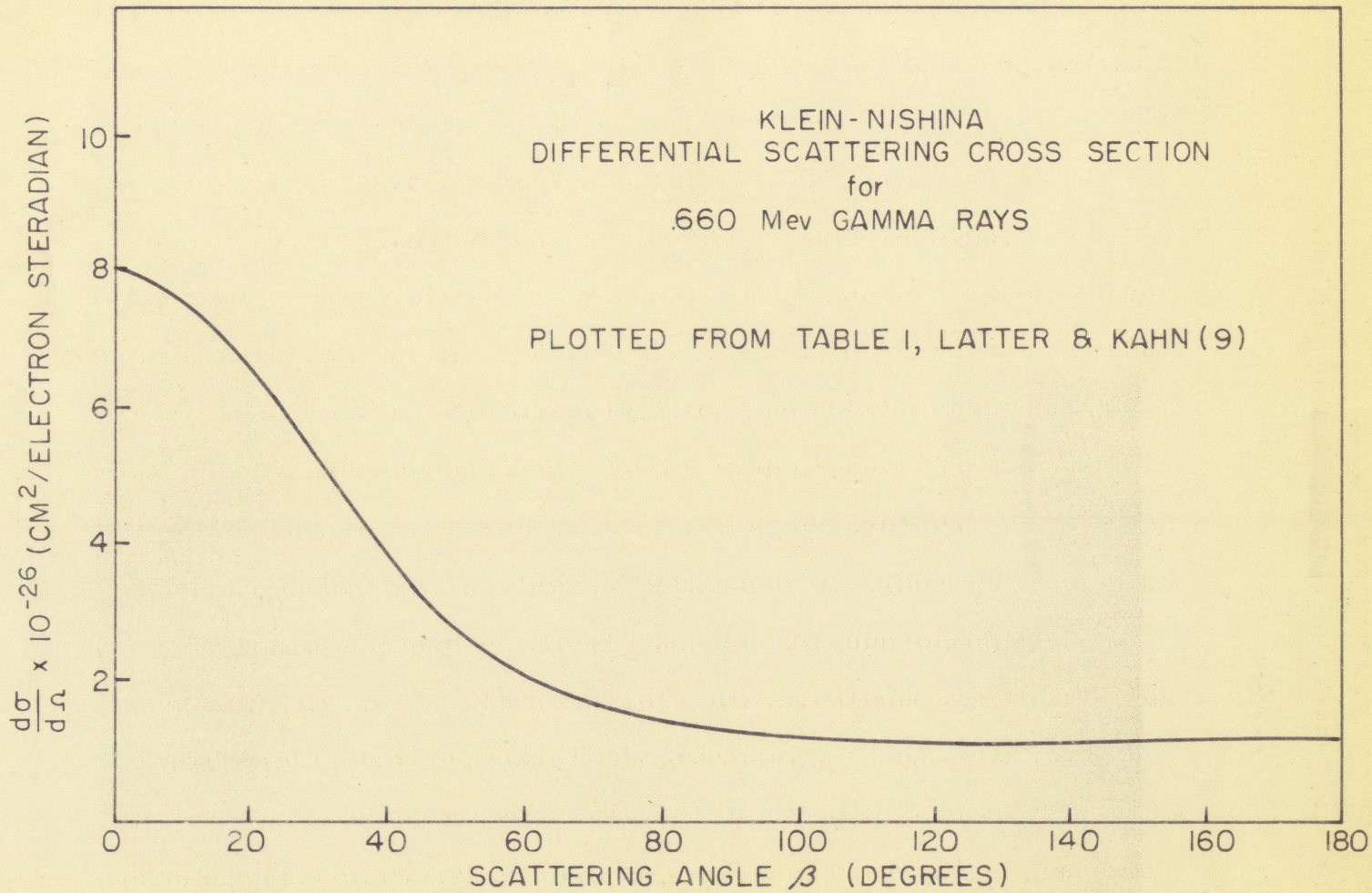

Figure 4. Variation in cross section with scattering angle

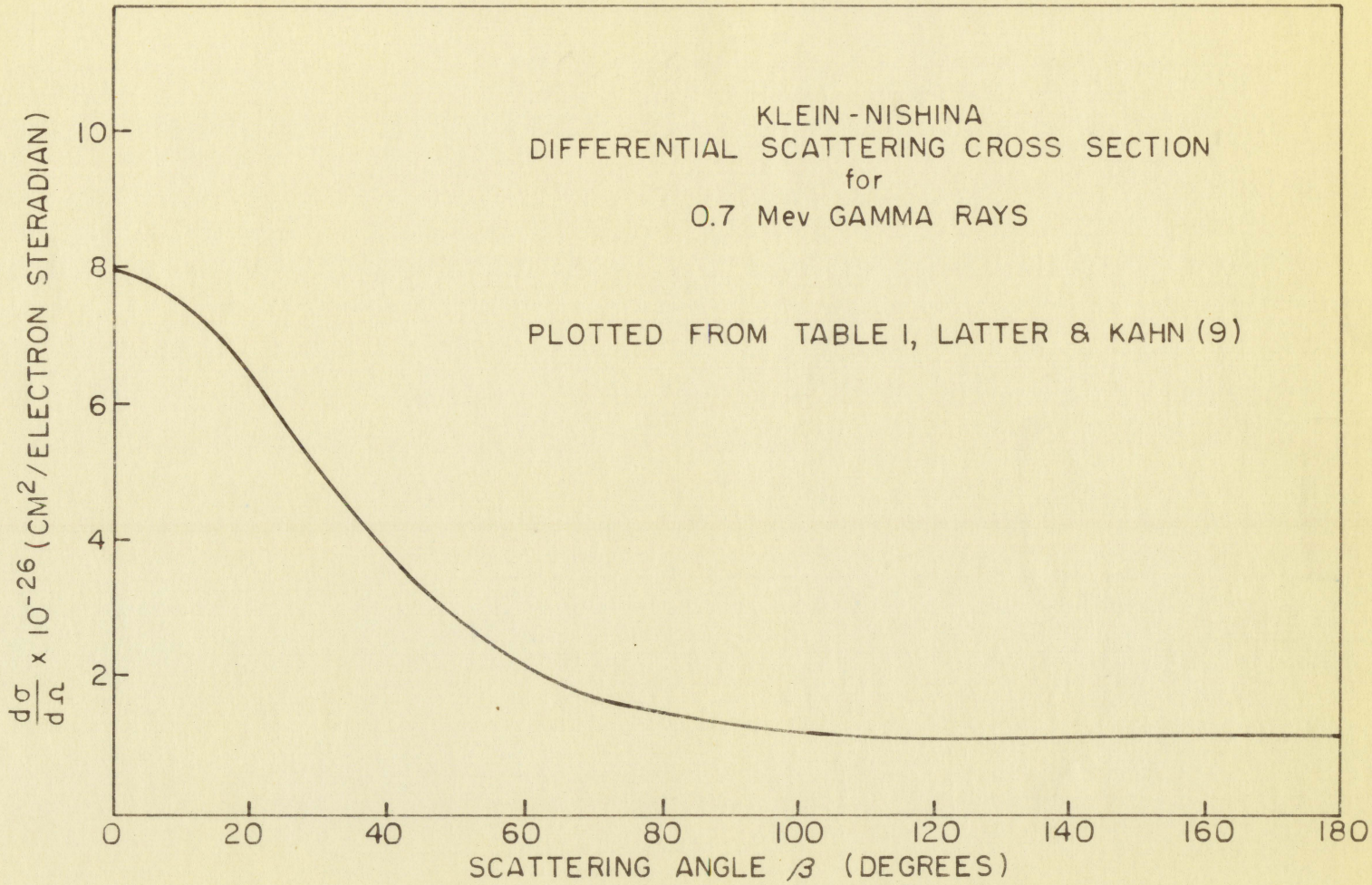

Figure 5. Variation in cross section with scattering angle

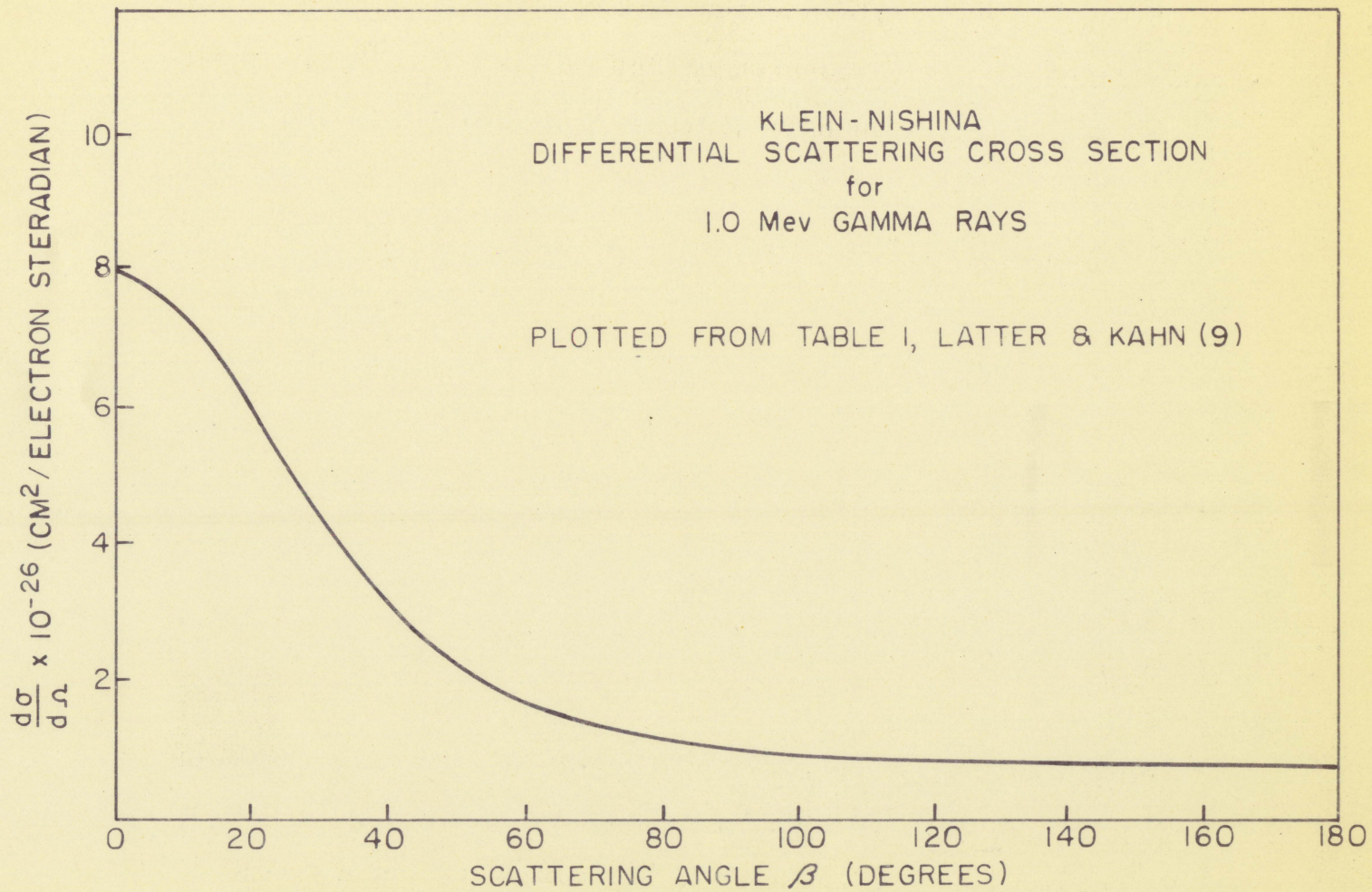

Figure 6. Variation in cross section with scattering angle

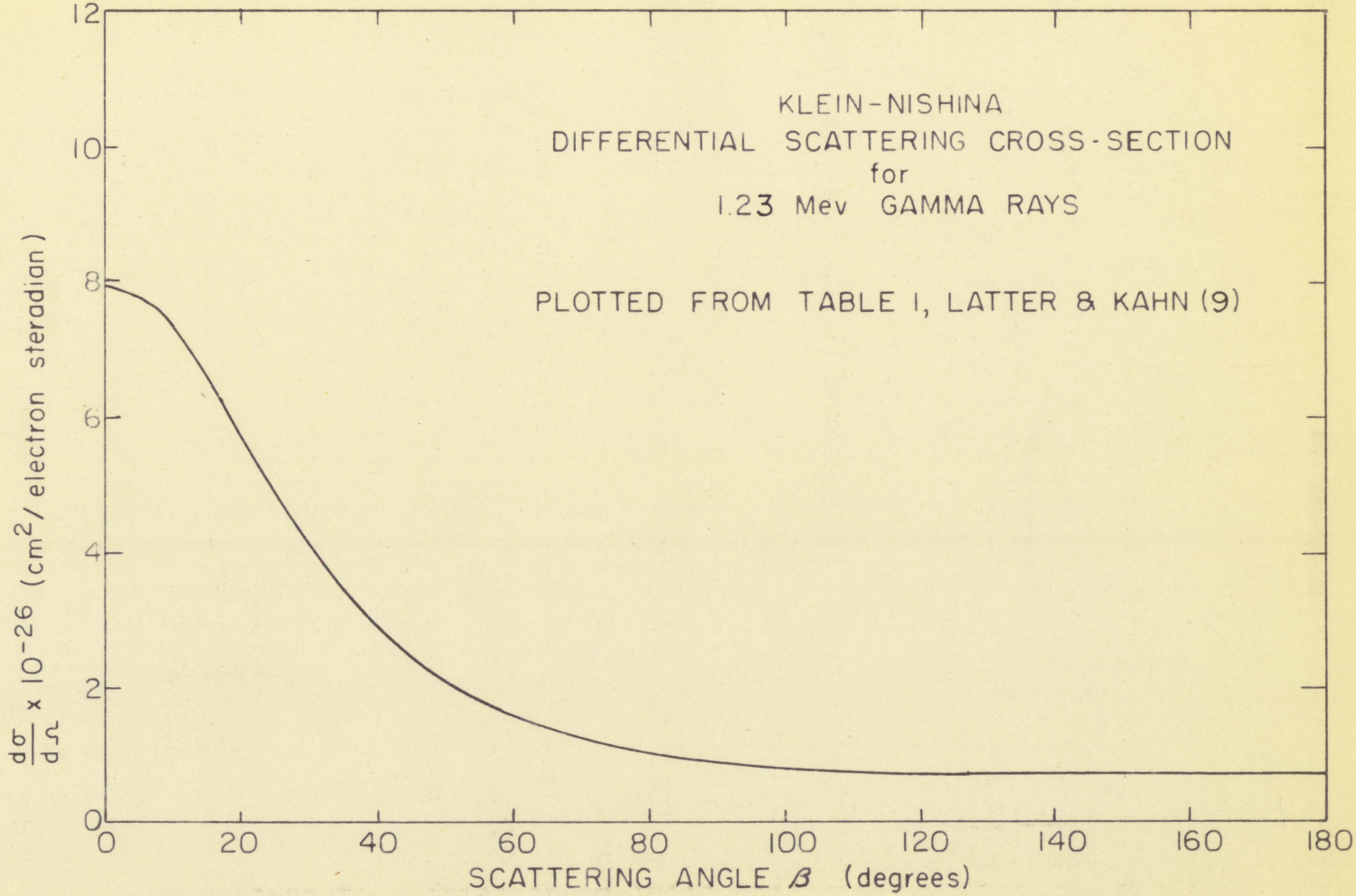

Figure 7. Variation in cross section with scattering angle

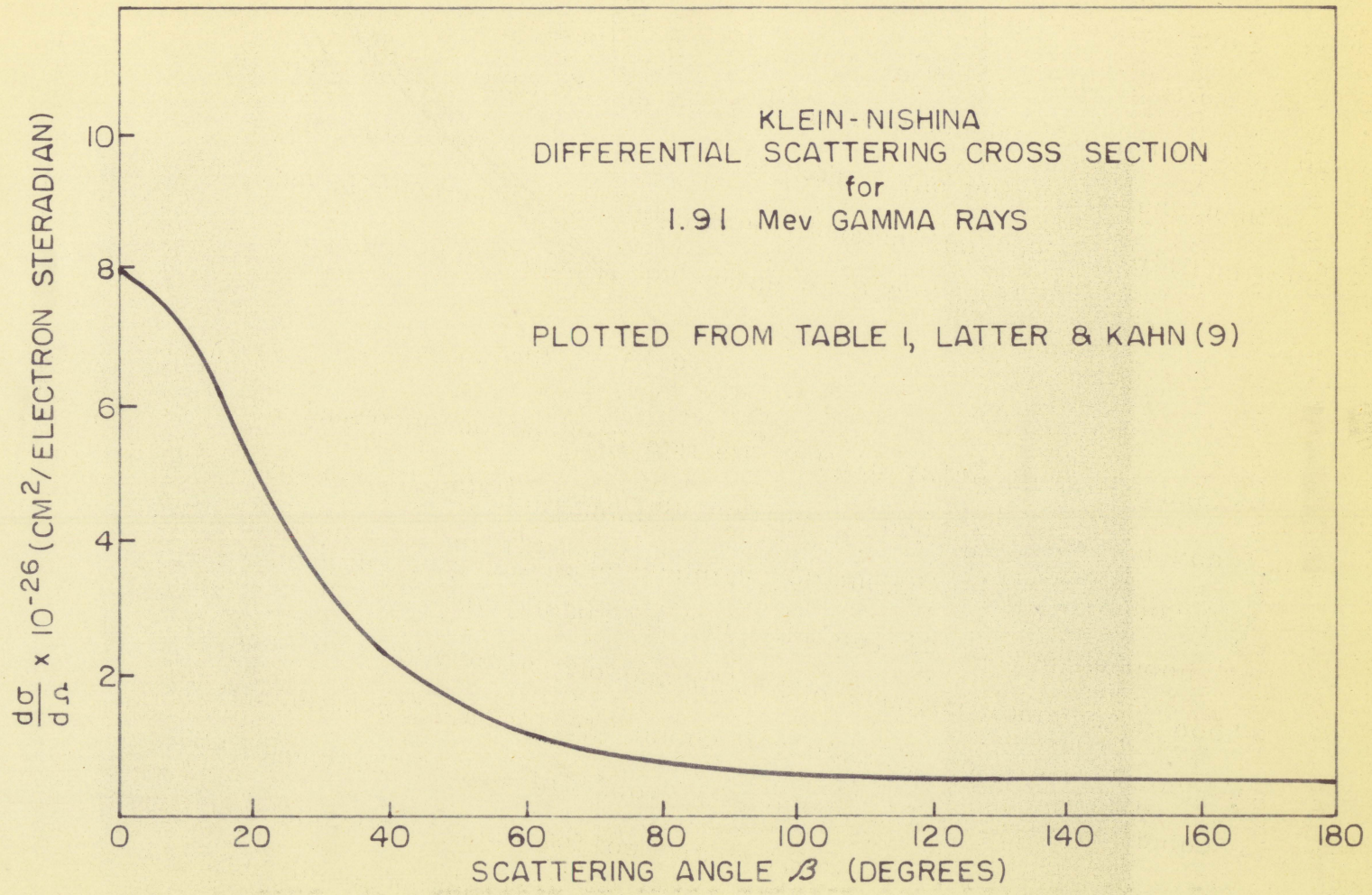

Figure 8. Variation in cross section with scattering angle

Energy (Mev)	Angle (degrees)
0.31	66.0
0.66	53.1
0.70	51.3
1.00	50.8
1.23	48.6
1.91	44.0

A still less obvious effect of scattering is the possibility that, as a result of the scattering process, the scattered photons would undergo an energy loss great enough to alter their coefficients of absorption and thus ultimately alter the extent of their absorption. This energy decrement results from the energy absorption of the recoil electrons, and in order to calculate the value of the loss the theory of multiple gamma scattering will be developed briefly.

To treat the contribution of the Compton effect to the attenuation of a beam of gamma rays in matter it is necessary to calculate the probability that such a scattering process will occur. An expression for this probability in terms of cross section ($_e\sigma$) per electron for the removal of photons from the incident beam by scattering is provided in the Klein-Nishina formula (8, p. 322):

$$_{e}\sigma = \frac{3}{4}\phi_{o}\left\{\frac{1+\alpha}{\alpha^{2}}\left[\frac{2(1+\alpha)}{1+2\alpha} + \frac{1}{\alpha}\ln(1+2\alpha)\right]\right.$$

$$\left. + \frac{1}{2\alpha}\ln(1+2\alpha) - \frac{1+3\alpha}{(1+2\alpha)^{2}}\right\}$$

where

$$\alpha = \frac{h\nu_{o}}{m_{o}c^{2}}$$

If $_{e}\sigma$ is multiplied by $\rho N(\frac{Z}{A})$, the Compton absorption coefficient σ (cm^{-1}), which has been previously used in attenuation calculations, results. However, in addition to σ's being a measure of the probability of a photon's being scattered out of the beam per centimeter of absorber, because of the beam's initial homogeneity, it is also a measure of the total amount of energy removed from the beam per centimeter of absorber (8, p. 332). This energy loss has two components: the amount of energy carried off by the scattered photons and the amount of energy absorbed by the recoil electrons symbolized by $_{e}\sigma_{s}$ and $_{e}\sigma_{a}$ respectively. The formula for $_{e}\sigma_{s}$ is (8, p. 333)

$$_{e}\sigma_{s} = \frac{3}{8}\phi_{o}\left\{\frac{1}{\alpha^{3}}\ln(1+2\alpha) + \frac{2(1+\alpha)(2\alpha^{2}-2\alpha-1)}{\alpha^{2}(1+2\alpha)^{2}}\right.$$

$$\left. + \frac{8\alpha^{2}}{3(1+2\alpha)^{3}}\right\}.$$

$_e\sigma_s$ can be changed to σ_s or the Compton scattering cross section per electron can be converted to the Compton scattering cross section by multiplying by $\rho N(\frac{Z}{A})$. Likewise, $_e\sigma_a$ can be converted to σ_a. Since the Compton absorption coefficient equals the sum of its two components of scattering and absorption,

$$\sigma = \sigma_s + \sigma_a$$

and since the Compton coefficient is given by Table 1, if $_e\sigma_s$ is found by the formula above and subtracted from the Compton coefficient, the Compton cross section for absorption (or the amount of energy removed from the beam through absorption by the recoil electrons) may be calculated (6, p. 328).

If a value of 6.651×10^{-25} cm^2 is used for ϕ_o, and the computation is carried out for 1.91 Mev (the highest energy photon to be treated in this paper), $_e\sigma_s$ in water is determined to be 52.7×10^{-2}. If this value is multiplied by $\rho N \frac{Z}{A}$, a value of 0.021 results for σ_s. This is compared to the 0.023 value from Table 1. The energy decrement of 0.002 may be ignored in these calculations. This same computation for uranium results in a calculated σ_s of 0.346 versus 0.340 of Table 1. Again this decrement produces a negligible effect on absorption.

Calculations of radiation values at the vertices will again be initiated with the source strength of 4.77×10^4

photons/cm^2-min. The photons from the source pass through the wooden cup (by which the source is positioned in the assembly), progress through the lattice, the water reflector, and finally through the steel shell to the detector. The photons in passing through the wooden cup are both scattered and absorbed by the wood. Reciprocal scattering takes place as the photons progress through the wood, and the number of photons scattered out of the vertex path therefore equals the number scattered in. The fact that those scattered in have undergone a change in direction, however, precludes their following the vertex path to the detector. As was indicated in previous calculations the average angle through which the photons are scattered ranges from 66° for the 0.31 Mev photon to 44° for the 1.91 Mev photon. When the photons in the vertex path reach the lattice, this change of direction of the photons scattered into the vertex path results in their progressing across this path and into the lattice rather than following the vertex path. As previous calculations indicate, the photons thus scattered into the lattice are absorbed there. Hence, scattered photons in this situation become lost to the system. Consequently when computing the absorption in the photon paths traversing the wood cup, the total attenuation coefficient is used. If, for the 1.91 Mev photon, the standard attenuation formula is employed with a total attenuation coefficient of 0.016 cm^{-1} from Table 1, the computation takes the form

$$R_1 = R_o e^{-\mu x}$$

This calculation results in the reduction of the value for the 1.91 Mev gamma-radiation to 1.15×10^4 cpm/cm^2. The radiation is further reduced as it progresses along the vertex path through the lattice by the intervening water. Again the same formula for attenuation is used and the total attenuation coefficient (0.048 cm^{-1}) is employed for the reasons given in the discussion of the attenuation by the wood. This calculation results in the level of radiation being reduced to 3.44×10^3 cpm/cm^2. As the radiation beam emerges from the lattice, it undergoes absorption and scattering by the water reflector. Since this path leads through a homogeneous medium (water), reciprocal scattering would be expected. However, since total absorption takes place in the lattice along paths C through H, there remains no radiation available to be scattered into paths A and B. Therefore, radiation that is scattered out at the vertex path by the water reflector is not reciprocated, so the total attenuation coefficient (0.048 cm^{-1}) is again employed in calculating the reduction of the radiation level. If the standard attenuation equation is again used the radiation level is computed to be reduced to 8.94×10^2 cpm/cm^2. A last attenuation caused by the quarter-inch steel shell of the assembly further reduces the value of the 1.91 Mev radiation in the vertex path to 8.05×10^2 cpm/cm^2.

It was previously indicated that the photons emerging

from the lattice along the vertex path are scattered by the water reflector. Since the average angle of scatter for 1.91 Mev photons was previously calculated to be 44°, this radiation is seen to be dispersed over a wide area. It is possible that this scattered radiation might contribute measurable values of radiation to points of measurement terminating paths other than those from the vertices. The probability of this radiation's scattering into a specific angle increment may be calculated from the tables of the differential cross section provided by Latter and Kahn (9, p. 9) and previously used to find the average angle of scatter. Graphs prepared from these tables are provided in Figures 3 through 8. The method of computation will require merely the comparison of an area of increment, e.g., 1°, with the total area, since the total area represents the total probability, or one.

From the previous results in the calculations of the average angle of scatter and from the shape of the differential scattering plot, it is evident that the scatter is preferentially forward and small-angle. Because of its small-angle nature the largest portion of the scattered radiation will be directed at the points closest to the path in which the scattering originated. Thus, the termination of path B should receive the greatest amount of the radiation scattered from path A. If the system of computation previously outlined for determining the probability of scattering into a specific angle is used, and the increment of the angle is 2.5° to 3.5°,

the probability of scatter into that increment is determined to be 2.46×10^{-2}. The radiation emerging from the lattice by the vertex path has been computed to equal 3.44×10^{3} cpm/cm^2. If the standard attenuation formula is used with the attenuation coefficient for Compton scattering for 1.91 Mev photons ($0.023 cm^{-1}$), the reduction due to scattering in the radiation path can be calculated. Hence, the amount of scattered radiation can then be found by subtracting from the original radiation the value of the scatter-attenuated radiation. As a result of these computations 1.63×10^{3} photons/cm^2-min are determined to be scattered by the water reflector. If this value is multiplied by the previously calculated probability of its being scattered into the angle increment of 2.5° to 3.5°, and then by the attenuation factor resulting from the water absorption along the scattered path, it is calculated that approximately 20 photons/cm^2-sec are scattered from path A to path B. Since this value is below background it may be ignored. Inasmuch as these calculations were made under conditions most favorable to scattering from path A to path B, all other path-to-path scatterings must be less likely to occur. Scattering in other paths and at other energies can therefore be ignored.

The attenuation of the gamma-rays of 1.23 Mev, 0.66 Mev and 0.31 Mev in the vertex path can be determined by a similar method of calculation. The following values are thus obtained:

Gamma energy (Mev)	Activity (cpm/cm^2)
1.91	8.05×10^2
1.23	3.61×10^2
0.66	6.40×10
0.31	1.90×10

Path B, though not a vertex path, is included in the vertex path analysis because the system of calculation employed in determining the attenuation of the radiation in path B is similar to that for the vertex path. This system of computation will again be initiated with a source strength of 4.77×10^4 photons/cm^2-min. The attenuation for the 1.91 Mev gamma-rays resulting from the path's traversing the wooden cup reduces the radiation to 1.15×10^4 cpm/cm^2. The radiation is further reduced as it progresses along path B by the intervening two inches of uranium. This reduction can be computed by the general attenuation formula in which the total attenuation coefficient (0.91 cm^{-1}) is employed for reasons mentioned in connection with the vertex path. A radiation value of 1.15×10^2 cpm/cm^2 results. The reduction by the remaining ten inches of water in the lattice can be computed by the use of the same attenuation formula and a total attenuation coefficient of 0.048 cm^{-1}. By this computation the radiation level is reduced to 34.9 cpm/cm^2. This value is below background. Moreover, the water outside the lattice and the steel shell would have provided still greater attenuation. The less energetic gamma-rays because of their higher

coefficients of absorption would be attenuated more quickly to a value below background in traversing the lattice through path B.

3. Source radiation pattern summary

As a result of the previously calculated attenuation processes, the following pattern of gamma-radiation is expected:

a. For paths through the lattice Radiation following paths through the lattice (B, C, D, E, F, G, and H) is attenuated to a value below that of background.

b. At the lattice vertices Radiation following paths from the lattice vertices (A) will be attenuated to the following values:

Gamma energy (Mev)	Activity (cpm/cm^2)
1.91	8.05×10^2
1.23	3.61×10^2
0.66	6.40×10
0.31	1.90×10
Total	1.249×10^3

Added to both of these predicted measurements is, of course, the contribution from the neutron multiplication, fission, and attendant gamma release in the lattice -- as yet uncalculated.

B. Origin and Diffusion of Fission Gamma Rays

In addition to the gamma radiation from the radium-beryllium source, the concomitant neutron emission causes fissioning in the lattice which in turn yields additional gamma radiation. A one-group analysis of the assembly is conducted to determine the fission gamma yield in the lattice.

1. Reactor analysis

The device employed in one-group theory is the four-factor formula which provides a method of obtaining the infinite multiplication factor K_∞. K_∞ is the ratio of the average number of neutrons produced in each generation to the average number of neutrons absorbed in the previous generation; and this quantity is used to calculate the effective multiplication factor, K_{eff}. K_{eff} is the ratio of the average number of neutrons produced by fission in each generation to the total number of neutrons absorbed in the previous generation by fuel, moderator, etc. K_∞ and K_{eff} are related to one another through the critical equation which will be the basis for subsequent calculations. In a reactor in which water is the moderator the critical equation takes the form (6, p. 189):

$$K_{eff} = \frac{K_\infty}{(1+L^2B^2)(1+L_1{}^2B^2)(1+L_2{}^2B^2)(1+L_3{}^2B^2)(1+L_4{}^2B^2)}$$

Thus, to find K_{eff}, values for K_∞, L^2 and B^2 must be determined.

a. K_∞, infinite multiplication factor As previously indicated, K_∞ is determined by the four-factor formula. This formula provides the following relationship (6, p. 179):

$$K_\infty = \eta \epsilon p f$$

Hence, to determine K_∞, each of the four factors must be evaluated. The individual factor determination will be effected in turn beginning with

1. η, neutron emission factor The neutron emission factor, η, is defined as the average number of fast (fission) neutrons emitted as a result of the capture of a thermal neutron in fuel (both U^{235} and U^{238}). This factor may be evaluated by the following formula (6, p. 178):

$$\eta = \frac{\nu N_5 \sigma_f}{N_5 \sigma_f + N_5 \sigma_{5_c} + N_8 \sigma_{8_c}}$$

where ν is the average number of fast neutrons released per slow neutron and equals 2.5 ± 0.1 (7, p. 83)

N_5 is the number of atoms of U^{235} per atom of natural uranium in the assembly and equals 0.007.

σ_f is the cross section for fission of the U^{235} and is equal to 549 (6, p. 109).

σ_{5_c} is the cross section for capture of the U^{235} and is equal to 101 (6, p. 109).

N_8 is the number of atoms of U^{238} per atom of natural uranium in the assembly and equals 0.9927.

σ_{8c} is the cross section for capture of the U^{235} and is equal to 2.8 (6, p. 109).

When these values are substituted in the formula for η and the indicated computation performed, a value for η of 1.31 results.

2. ϵ, fast fission factor The fast fission factor, ϵ, is defined as the ratio of the total number of fast neutrons produced by fissions due to neutrons of all energies (fast and thermal) to the number resulting from thermal-neutron fissions. When a hexagonal cell of the given lattice is converted into an equivalent cylindrical cell, a value of 0.91 in. is obtained for the equivalent radius. With this value of equivalent radius, a fast fission factor of 1.028 is determined from plotted calculations by Glasstone for heterogeneous reactors (6, p. 195).

3. p, resonance escape probability factor The resonance escape probability factor is defined as the fraction of the fast (fission) neutrons which escape capture while being slowed down. The resonance escape probability factor may be calculated by the method developed in the Reactor Handbook (12).

$$P = \exp\left[\frac{-A}{\xi \sigma_s}\right] \qquad \text{(12, p. 481)}$$

and $$\int \sigma_{a_{eff}} \frac{dE}{E} = A\mu \frac{S}{M} \qquad \text{(12, p. 481)}$$

therefore, $$A = \int \sigma_{a_{eff}} \frac{dE}{E} - \mu \frac{S}{M}$$

but, $$A = \int \alpha(E) \frac{dE}{E} = 9.25 \text{ barns} \qquad \text{(12, p. 497)}$$

and $$\mu = \int \beta(E) \frac{dE}{E} = 24.7 \frac{\text{barns-gm}}{\text{cm}^2} \qquad \text{(12, p. 497)}$$

And since

$$\frac{S}{M} = \frac{\text{Surface}}{\text{Mass}}$$

$$\frac{S}{M} \text{ (for cylinder)} = \frac{2}{r_o \rho} = 0.083$$

and $$\sigma_{a_{eff}} \frac{dE}{E} = A + \mu \frac{S}{M}$$

therefore, $$\sigma_{a_{eff}} = 9.25 + 2.05 = 11.3 \text{ barns}$$

Since $$\overline{\xi \sigma_{s_{H_2O}}} = 38.5 \qquad \text{(12, p. 498)}$$

and since

$$p = \frac{\sigma_{a\,eff}\ \frac{dE}{E}}{\xi\ \sigma_s}$$

$$= - \frac{11.3}{38.5}$$

$$p = 0.745.$$

Therefore, the resonance escape probability factor is equal to 0.745.

4. f, thermal utilization factor The thermal utilization factor, f, is defined as the ratio of the thermal neutrons absorbed in fuel to the total number of thermal neutrons absorbed by fuel, moderator and other materials present in the reactor. This ratio may be expressed in the formula (12, p. 480)

$$\frac{1}{f} - 1 = F(K_0 r_0) \left(\frac{\Sigma_U V_U}{\Sigma_{H_2O} V_{H_2O} + \Sigma_{Al} V_{Al}} \right)^{-1} + X(K_2 r_1', K_2 r_2)$$

where Σ_U is the macroscopic cross section for absorption in uranium. It is found by the formula

$$\Sigma_U = \frac{\sigma_U \rho_U N_A}{A_U}$$

where, in turn, σ_U is the microscopic cross section for absorption for natural uranium and equals $\frac{(650)(.007)}{225} + \frac{(2.8)(.993)}{238}$ with the cross sectional values of 650 b. and 2.8 b. from Glasstone (6, p. 109).

ρ_U is the density of natural uranium and is equal to 19 gm/cm^3.

N_A is Avogadro's Number and is equal to 6.023×10^{23}.

A_u is the atomic weight of uranium.

In this manner Σ_u is computed to be 0.366 cm^{-1}. In the formula for f,

V_u is the volume of uranium in the fuel cell and is equal to 5.17×10^2 cm^3.

Σ_{H_2O} is the macroscopic cross section for water, and by calculations similar to that for uranium, is determined to be 0.022 cm^{-1}.

V_{H_2O} is the volume of water in the fuel cell and is equal to 13.09×10^2 cm^3.

Σ_{AL} is the macroscopic cross section for aluminum and is computed to be 0.0126 cm^{-1}.

While V_{AL} is the volume of aluminum in the fuel cell and is equal to 7.53 x 10 cm3,

r_o is the radius of the uranium rod and equals 1.27 cm.

r_1 is the radius of the uranium rod with its cladding and equals 1.346 cm.

r_2 is the effective outer radius of the equivalent cylinder and equals 2.32 cm.

K_o is the reciprocal diffusion length of fuel and equals 0.646 cm^{-1} (12, p. 487).

K_2 is the reciprocal diffusion length of moderator and equals 0.35 cm^{-1} (12, p. 487).

P is the ratio of the thermal neutron density at the

surface of the uranium rod to the average thermal neutron density of the rod and is equal to 1.075 (12, p. 517).

X measures the excess neutron absorption in the moderator due to the excess density in the moderator over that of the moderator air interface. This quantity equals 0.05 (12, p. 519).

Upon proper substitution and performance of indicated operations, the thermal utilization, f, is determined to be 0.756.

But in the original equation for K_∞,

$$K_\infty = \eta \epsilon p f$$

The computed values for the four factors may therefore be substituted into the previous equation to yield a value for K_∞ of 0.747.

b. L, diffusion length The diffusion length, L, is described physically as one-sixth of the mean square distance that a thermal neutron would travel from the point at which it just becomes thermal to capture. Its value can be calculated by (6, p. 201)

$$L^2 = L_m^2 (1-f)$$

and its components may be determined in the following manner:

1. f, thermal utilization factor This quantity was previously determined to be 0.756.

2. L_m, diffusion length of the pure moderator

The diffusion length of a water moderator as determined by Glasstone to be 2.88 cm (6, p. 144).

Therefore, L^2 is calculated by the preceding formula to be 2.02 cms. L_1, L_2, L_3 and L_4 have been experimentally determined by Glasstone as 4.49, 2.45, 2.05, and 1.00 cms respectively (6, p. 145).

c. B^2, buckling The remaining factor to be provided the critical equation is B^2, or the buckling factor. Buckling may be thought of as a parameter relating size and composition in the reactor. To determine this factor for the subcritical reactor of interest in this paper, some macroscopic reactor theory for heterogeneous (natural uranium) reactors must be developed. Generally, this development will be patterned on that of Glasstone and Edlund (7, pp. 285-289).

To be able to employ this system of analysis, however, it must be determined that the neutrons leaving the source are quickly thermalized so the activation measurements that are utilized in the analysis will have been made with thermal neutrons.

If a point source of n_o neutrons of energy E_o per second is assumed, the number that become thermal per second in a unit volume a distance r away is (10, p. 282)

$$q = n_o e^{-\frac{(r^2/4 L_f^2)}{(4\pi L_f)^{3/2}}}$$

where L_f is the fast diffusion length, and $L_f^2 = \tau$ (Fermi age). But,

$$\overline{r^2} = \frac{\int r^2 \, q \, dV}{\int q \, dV} \qquad \text{(10, p. 282)}$$

and $\overline{r^2} = 6 L_f^2$.

Therefore, for water

$L_f^2 = 33 \text{ cm}^2$ (10, p. 282)

$6L^2 = 198$

rms = 14 cms.

This root mean squared distance represents the slowing down distance described in b above. In experimental measurements, however, the distance r proves to be greater than the calculated distance. Murray (10, p. 282) has determined a value of 30 cms for the slowing down distance. In any event, it is evident that the neutrons are rapidly slowed in the water moderator.

With this evidence of the rapid thermalization of the source neutrons, a return to the reactor analysis is made. The solution of the wave equation for the neutron diffusion in a cylindrical reactor is found to be separable into the

product of a function in r, $A(r)$, and z, $Z(z)$. Thus the wave equation takes the form (7, p. 286):

$$f\left[A(r)\right] + f'\left[Z(z)\right] + B_m^2 = 0$$

from which the buckling B_m^2 is to be calculated.

If $A(r)$ is represented by the constant $-\alpha^2$ and $Z(z)$ by $-\gamma^2$ where both constants are positive, then (7, p. 286)

$$\alpha^2 - \gamma^2 = B_m^2 .$$

The solution in A becomes (7, p. 286):

$$A(r) = \sum_{n=1}^{\infty} A_n J_o(\alpha_n r) \quad n = 1, 2 \ldots$$

and the solution in Z is (7, p. 286)

$$Z_n = C_n \sinh \gamma_n (H - z)$$

where H is the extrapolated height. The general solution of the wave equation is now (7, p. 287)

$$\phi(r, z) \sum_{n=1}^{\infty} A_n J_o(\alpha_n r) \sinh \gamma_n (H - z)$$

so that at the bottom of the face of the cylindrical pile,

$$\phi(r, o) = f(r) \quad \text{and} \quad f(r) = \sum_{n=1}^{\infty} A_n^1 J_o(\alpha_n r)$$

But if only the fundamental term is used, the general solution reduces to (7, p. 287)

$$\phi = A J_o(\alpha r) \sinh \gamma (H - z)$$

It is evident that values for α and γ must be calculated in order to solve for buckling. The value of γ will be determined first.

Since (if only the fundamental term is used)

$$\phi(z) = A' \sinh \gamma (H - z)$$

The extraction of the exponential term takes the form (7, p. 287),

$$\phi(z) = C e^{-\gamma z} \left[1 - e^{-2\gamma(H-z)} \right]$$

A value of γ can be obtained by employing the following procedure. The neutron flux is measured at various distances from the bottom of the assembly in a vertical line parallel to the z-axis. The extrapolated height, H, is determined, and the slope, $-\gamma$, of the plot of the logarithm of the exponential flux, in $\phi(z)$, against the vertical distance z, can be obtained. The data for such a plot, included in Appendix B, were made available from the activation experiments conducted by Dr. Robert Uhrig of the Department of Theoretical and Applied Mechanics, Iowa State College (14). From these activation data the necessary relationships of quantities are included in Table 2, and a plot of values is provided in Figure 10.

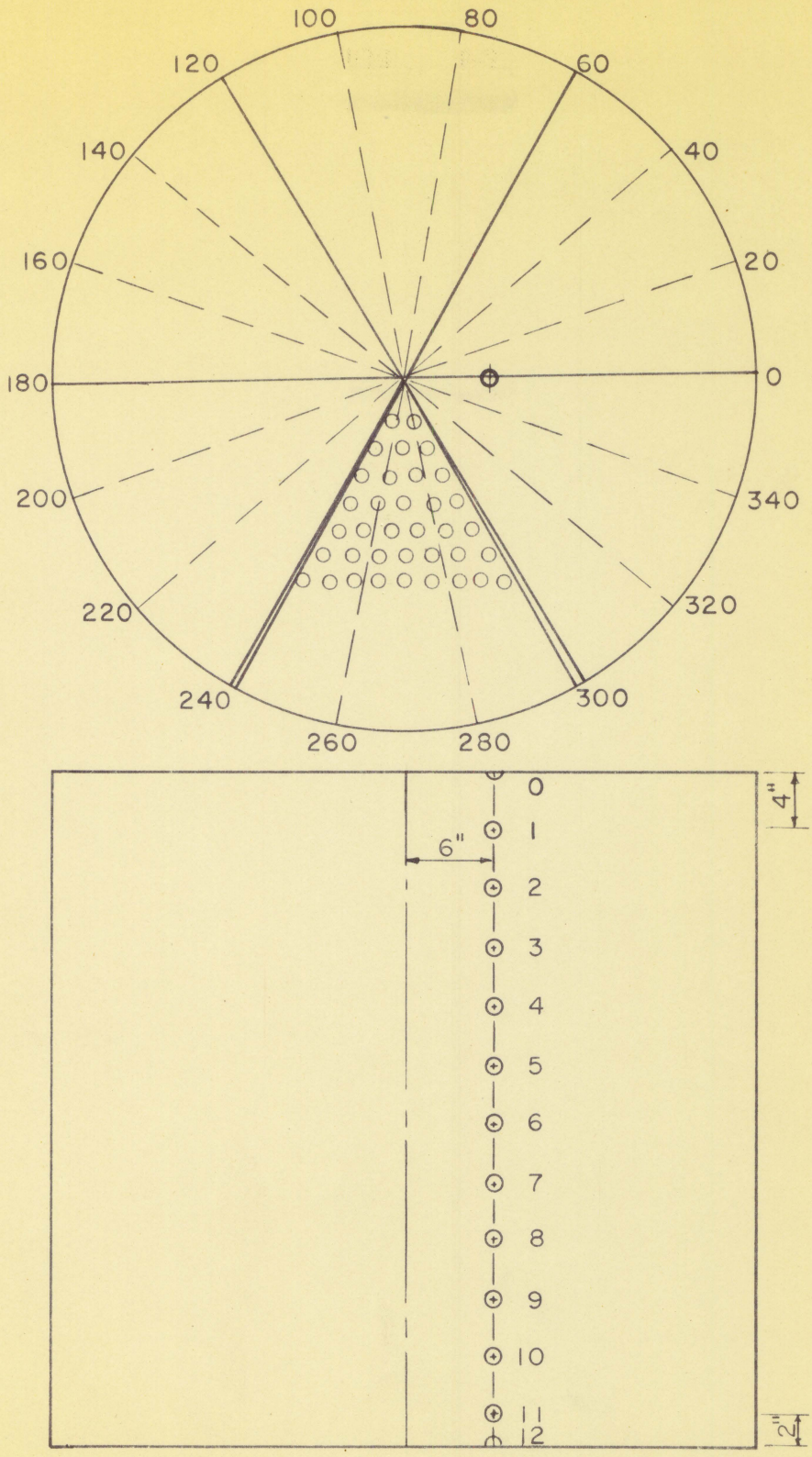

Figure 9. Location of points of neutron measurement

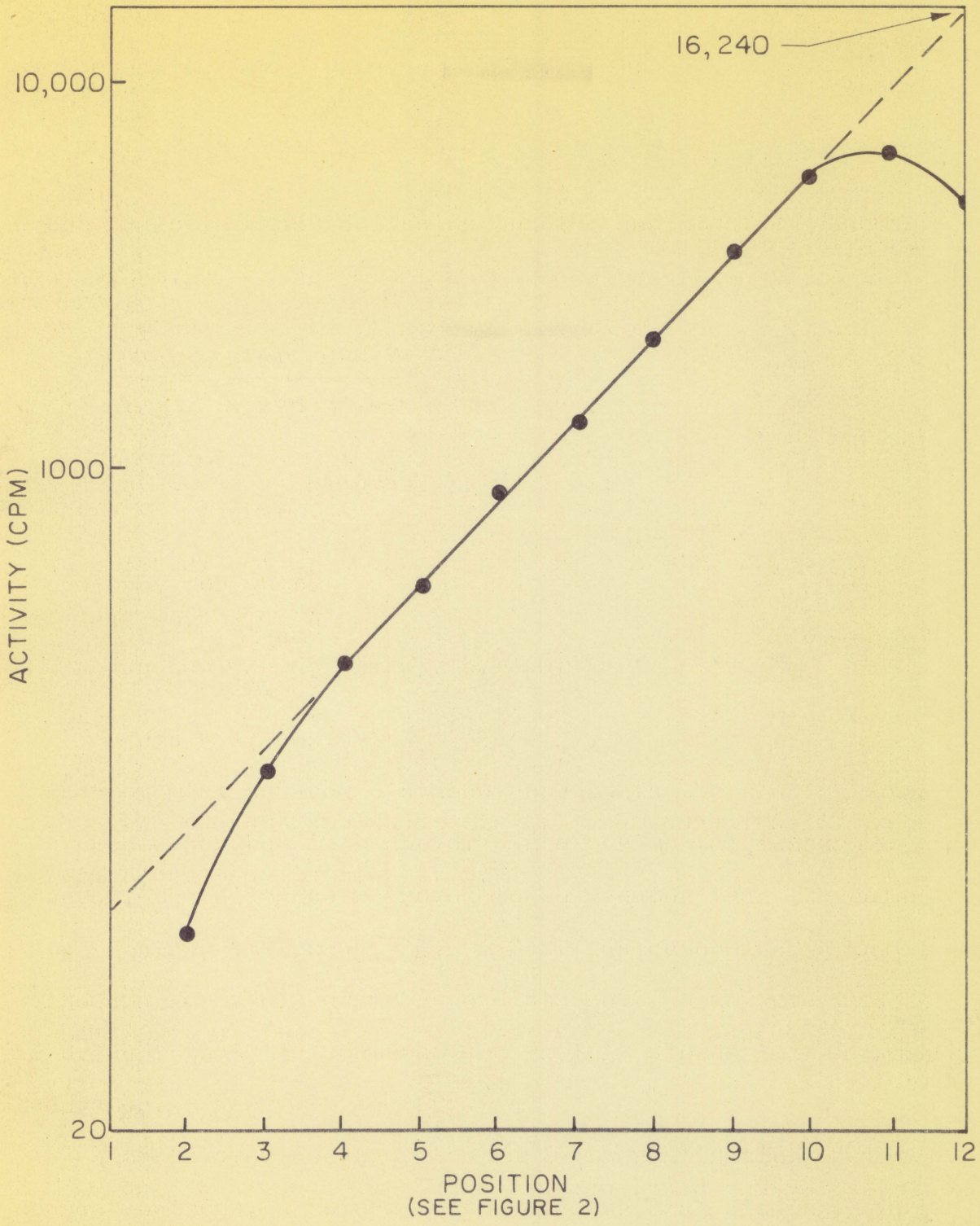

Figure 10. Experimental neutron data for determining buckling

Table 2. Results of activation experiments

Position	ϕ/ϕ_o	$\ln \phi/\phi_o$	z (cms)	$\ln \phi/\phi_o / z = \gamma$
4	0.0196	-4.280	24	0.1785
5	0.0312	-3.470	21	0.1650
6	0.0550	-2.900	18	0.1610
7	0.0821	-2.500	15	0.1665
8	0.1361	-1.990	12	0.1660
9	0.2290	-1.480	9	0.1645
10	0.3590	-1.025	6	0.1710

Therefore,

$$\Sigma \ln \phi/\phi_o / z = 1.1725 \text{ in}^{-1}$$

$$\text{Avg } \ln \frac{\phi/\phi_o}{z} = 0.1675.$$

Therefore, since

$$\gamma = 0.1675 \text{ in}^{-1}$$

$$\gamma = 0.0658 \text{ cm}^{-1}$$

and $$\gamma^2 = (6.58 \times 10^{-2})^2 = 43.0 \times 10^{-4} \text{ cm}^{-2}$$

which is one of the quantities needed in the calculation of buckling.

The remaining quantity necessary for the determination of buckling is the constant α^2. From the general solution of the wave equation (7, p. 287),

$$\phi = A J_0 (\alpha r) \text{ Sinh } \gamma (H - z).$$

The expression for A (r) becomes (7, p. 287)

$$A(r) = A J_0 (\alpha r).$$

And from the boundary condition that the flux shall be zero at the (extrapolated) surface of the lattice (7, p. 287)

$$\alpha = \frac{2.405}{R}$$

where R is the extrapolated radius.

To find R and ultimately α, several quantities must be calculated, the first of which is

1. Σ_s, macroscopic scattering cross section for water The macroscopic cross section of water can be determined from the relationship (6, p. 92)

$$\Sigma_s = \frac{\rho_{H_2O} N_A (2\sigma_{s_H} + \sigma_o)}{A_{H_2O}}$$

where σ_{s_H} is the microscopic cross section for scatter of hydrogen, and is equal to 46 b. (15, p. 135)

σ_{s_o} is the microscopic cross section for scatter of oxygen, and is equal to 4.2 b. (6, p. 841)

ρ_{H_2O} is the density of water and equals one.

N is Avogadros's number and equals 6.023×10^{23}, and A_{H_2O} is the atomic weight of water and equals 18. A value for Σ_s of 3.22 cm^{-1} is obtained by making the proper substitutions and carrying out the indicated operations.

2. $\bar{\mu}_o$, average cosine of scattering angle The average cosine of scattering angle, $\bar{\mu}_o$, can be approximated

by (7, p. 98)

$$\bar{\mu}_o = \frac{2}{3A}$$

where A is the atomic weight of water and is equal to 18. Therefore $\bar{\mu}_o = 0.037$.

3. λ_t, transport mean free path The transport mean free path is described by the relationship (7, p. 98):

$$\lambda_t = \frac{1}{\Sigma_s (1 - \bar{\mu}_o)}$$

If the previously calculated quantities of Σ_s and $\bar{\mu}_o$ are substituted into this expression, values of λ_t equal to 0.323 and $0.71\,\lambda_t$ equal to 0.229 are obtained.

But $R = R_o + 0.71\,\lambda_t$ (7, p. 288) and R, therefore, is equal to 61.229 cms. And since

$$\alpha = \frac{2.405}{R},$$

α is equal to 0.0392 cm^{-1}. Thus α^2 must equal 15.3×10^{-4} cm^{-2}.

In the original relationship of the constants from the wave equation,

$$B_m^2 = \alpha^2 - \gamma^2$$

If the calculated values of α^2 and γ^2 are substituted, a value for B_m^2 of -27.7×10^{-4} cm^{-2} is obtained.

The preceding calculation was made in an attempt to calculate K_{eff}. However, B^2 is found to be negative, and if

this negative quantity is substituted into the critical equation, a K_{eff} greater than K_∞ will result. But by definition K_∞ must be greater than K_{eff}, since K_∞ is the reproduction constant under ideal conditions.

It is evident then that either numerical or experimental errors invalidate the results or the critical equation is not applicable. The critical equation is arrived at by solving simultaneously the Fermi Age equation and the diffusion equation. The result of this operation takes the form: (7, p. 198)

$$K_{eff} = \frac{K_\infty \quad e^{-B^2 \tau}}{1 + L^2 B^2}$$

Since the moderator is water and the slowing down is accomplished in single-collision processes postulated by the Fermi Age theory, τ equals zero, and the critical equation may be written as

$$K_{eff} = \frac{K_\infty}{1 + L^2 B^2}$$

This equation has been further modified by Glasstone (6, p. 189) in view of experimental data to take the form shown on p. 30 of this thesis. It is evident therefore that the value of K_{eff} is dependent only on the solution of the diffusion equation. This equation may be written as (7, p. 101)

$$D \nabla^2 \phi - \Sigma_a \phi + S = \frac{\partial n}{\partial t}$$

If the equation is divided by D, it becomes

$$\nabla^2 \phi - \frac{\Sigma_a \phi + S}{D} = \frac{1}{D} \frac{\partial n}{\partial t}$$

If $B^2 = \frac{-\Sigma a + S}{D}$,

then the sign of B^2 will be dependent upon the relative magnitude of the absorption term and the source term. If one neutron is assumed to have been absorbed, then the number of neutrons produced by that absorption is represented by the previously calculated K_∞. The value of K_∞ was computed to be 0.747. If these values are substituted into the expression for B^2

$$B^2 = \frac{-1 + 0.747}{D}$$

B^2 is thus seen to be negative. In order to apply the simple diffusion theory, the medium in which the diffusion takes place must be a poor absorber (6, p. 92). This condition is necessary, for in the development of the diffusion equation, Σ_{total} is replaced by Σ_s. This approximation is only valid when the diffusing medium is a poor absorber. The absorbing properties of water may be seen in the following development.

The path length followed by the neutron will be given by $\lambda_s N$, where N equals the total number of collisions as the neutron traverses the lattice and λ_s equals the mean free

path for scattering. An approximation for the "random walk" process of this path can be written

$$d = (\overline{l^2}N)^{\frac{1}{2}}$$

where d equals the rms displacement from the source and $(\overline{l^2})^{\frac{1}{2}}$ approximates λ_s, the mean free path for scattering.

If $d = \lambda_s N^{\frac{1}{2}}$,

then $N = \frac{d^2}{\lambda_s^2}$

and the actual path length $\lambda_s N = \frac{d^2}{\lambda_s}$.

The attenuation of neutrons through x thickness of material can be expressed (7, p. 96)

$$I_x = I_o e^{-x\Sigma_a}$$

where Σ_a is the macroscopic cross section for absorption for water, and has been previously calculated to equal 0.022 cm^{-1}. The attenuation for a 10-cm path in water can be calculated as follows:

$$\frac{I_x}{I_o} = e^{-\Sigma_a x},$$

and $$D = \frac{\lambda t}{3}$$

or $$\lambda t = 3D$$

But, $\lambda t \approx \lambda_s$,

therefore, $\lambda_s = 3D$

where D is the diffusion constant and equals 0.142 cm (7, p. 127). Therefore,

$$\frac{I_x}{I_o} = e^{(-0.022)\ (10^2/3 \times 0.142)}$$

$$\frac{I_x}{I_o} = e^{-5.17}$$

$$\frac{I_x}{I_o} = 0.005$$

The attenuation in the 10 cm of water is therefore 0.005. If the same calculation is made for graphite, (with D equal to 0.903 cm and Σ_a equal to 0.00036 cm^{-1} from 7, p. 127)

$$\frac{d^2}{\lambda s} \quad \frac{100}{3 \times 0.903} = 37$$

$$\frac{I_x}{I_o} = e^{-0.00036 \times 37} = e^{-0.0133}$$

$$\frac{I_x}{I_o} = 0.987$$

The contrast in the absorption effect between a water and a graphite moderator is immediately obvious.

It is evident then that the highly absorptive nature of the water moderator precludes the use of the simple diffusion theory in calculations concerned with diffusion in a water moderator and a fuel of natural uranium. Therefore, the

correction to K_∞ ordinarily supplied by the buckling term of the diffusion equation is not available, and K_∞ is used as a first approximation for the reproduction constant.

2. Reactor source components

The efficiency of the reactor in regard to neutron economy in the fission process is approximated by the value of K_∞. This approximation of neutron conservation will provide an index to the number of fissions occurring and, hence, the gamma yield resulting from this process. The ordinary yield of prompt gamma radiation per fission amounts to approximately five photons at 1 Mev energy (6, p. 114). The total energy of delayed gamma radiation is found to be approximately 6 Mev (6, p. 22) with the mean energy of the delayed photons approximately 0.7 Mev (6, p. 119). Thus, the gamma yield would approximate 5 (1.0 Mev photons) and 8.5 (0.7 Mev photons) per fission. To determine the number of fissions several quantities must be computed, namely:

a. l_o, infinite median lifetime The infinite median lifetime, l_o, is described by the expression (7, p. 203):

$$l_o = \frac{\lambda_a}{v} = \frac{1}{\Sigma_a v}$$

where Σ_a is the macroscopic cross section for absorption and has previously been computed to be 0.022 cm^{-1}, and v is

the most probable velocity of thermal neutrons and equals 2.2×10^5 cm/sec (10, p. 37). By use of the above formula, λ_o is computed to be 2.065×10^{-4} seconds. Because of the failure of the diffusion equation in this case, the quantity λ_o cannot be modified to provide l, the finite median lifetime. However, this quantity (2.065×10^{-4} seconds) also represents the generation time (7, p. 203); and, therefore, if the number of neutrons produced each generation could be determined, the total number produced in a specific time interval could be computed. By definition, K_∞ represents that portion of the flux entering an assembly that remains after the scattering, absorption, and fissioning processes have taken place. Thus, if the original neutron flux from the source is known, at the end of the first generation, 0.747 of this number remains to initiate the second generation, and 0.747 of that number will remain to initiate the third generation, etc. After the tenth generation the subsequent contribution by later generations will not be significant. Hence, the sum of 32 generations should provide a good approximation of the neutron yield each second as a result of the neutron multiplication in the lattice.

If ϕ_o represents the original neutron emission from the radium-beryllium source, then the sum of the infinite series

$$\phi_t = \phi_o \frac{1}{1 - K_\infty}$$

(where $K_\infty = 0.747$)

equals an approximation of the total neutron yield. To compute this neutron yield then, it is necessary to determine the original neutron strength being generated by the (α , n) reaction in the source. If a value of 460 neutrons per 10^6 disintegrations is assumed (5, p. 108), a source strength of 100 millicuries should provide a neutron flux of 1.7×10^6 neutrons/sec. If this value is substituted for ϕ_o in the previous equation, ϕ_t is determined to be 7.15×10^6 neutrons/sec. Since approximately 2.5 neutrons are generated as a result of each fission, the number of fissions necessary to produce 5.45×10^6 neutrons/sec is seen to be 2.17×10^6. And since 5 (1.0 Mev) and 8.5 (0.7 Mev) photons are produced in each fission, evidently the total gamma yield from the lattice fissioning amounts to 10.85×10^6 (1.0 Mev) and 18.5×10^6 (0.7 Mev) photons/sec.

3. Reactor radiation calculations

a. S_v, volumetric source term With this value of total gamma emission, a volumetric source term can be computed by dividing the total gamma yield by the total volume of assembly. The volume of the assembly is determined to be 3.67×10^5 cm^3. Therefore, the average volumetric source term can be expressed

$$\text{Avg } S_v = \frac{10.85 \times 10^6}{3.67 \times 10^5} \text{ (1.0 Mev)} \quad \frac{18.5 \times 10^6}{3.67 \times 10^5} \text{ (0.7 Mev) photons/cm}^3\text{-sec}$$

b. S_a, surface source term This source can be changed into a surface source utilizing the relationship (6, p. 603):

$$S_a = S_v \lambda$$

where

$$\lambda = \frac{1}{\mu}$$

and μ is the coefficient of absorption.

The quantity $\frac{\mu}{\rho}$ for both 0.7 Mev and 1.0 Mev photons is determined to be 0.078 and 0.063 respectively by interpolation from values provided by Glasstone (6, p. 78). Values of 1.65 and 2.54 for the value of λ for 0.7 Mev and 1.0 Mev photons respectively are obtained if the reciprocal values for $\frac{\mu}{\rho}$ are divided by the density.

When these values are substituted in the equation $S_a = S_v \lambda$ previously provided, the following surface absorption term results:

$S_a = 4.89 \times 10$ (1.0 Mev) + 1.28×10^2 (0.7 Mev) photons/cm^2-sec

or for a longer period,

$S_a = 2.94 \times 10^3$ (1.0 Mev) + 7.67×10^3 (0.7 Mev) photons/cm^2-min.

In the remaining 11 inches of water, using an absorption coefficient 0.033 cm^{-1} (from Table 1), the radiation is reduced to 1.18×10^3 (1 Mev) and 3.07×10^3 (0.7 Mev) photons/min-cm^2. The steel shell further reduces the radiation to

1.18×10^3 (1.0 Mev) and 2.70×10^3 (0.7 Mev) photons/min-cm^2. Thus, everywhere on the periphery of the assembly the radiation level is increased 3.88×10^3 cpm/cm^2.

4. Reactor radiation pattern summary

At all points of measurement the contribution to the measured activity resulting from the reactor gamma-radiation would equal 3.88×10^3 photons/min-cm^2.

C. Theoretical Radiation Summary

The radiation from the radium beryllium source combines with the radiation resulting from fission to form the pattern described in Table 3.

Table 3. Computed radiation activities

Location	Path	Activity (cpm/cm^2)
Vertex	A	5.129×10^3
Intermediate point[a]	B	3.88×10^3
	C	3.88×10^3
	D	3.88×10^3
	E	3.88×10^3
	F	3.88×10^3
	G	3.88×10^3

[a]The interval between C, D, E, F, and G is 5°. The interval between A and B, as well as B and C, is 2.5°.

V. EQUIPMENT

A. Assembly

1. General description

The subcritical assembly upon which this radiation analysis was made consisted of a hexagonal lattice mounted in a cylindrical tank of light water as depicted in Figure 1. The actual location of the lattice with respect to its position in the cylinder is evident from Figure 11 in which the locations of the uranium columns in the spacer are shown. The height to which these columns reached is evident from Figure 12. The supporting shell was made from quarter-inch low-carbon steel.

2. Lattice

The lattice was hexagonal, consisting of 864 slugs of natural uranium canned in aluminum jackets with 1-3/4 inches between center lines. Each slug was one inch in diameter, eight inches long, and weighed approximately four pounds. Vertically, the slugs were arranged in four layers by quarter-inch aluminum spacer plates as depicted in Figure 1.

3. Moderator

The moderator of the assembly consisted of three hundred gallons of light water. With the steel shell, the water also

acted as a radiation shield. There was no provision for automatic makeup of evaporated moderator, but since access to the assembly was easily afforded, manual makeup as needed was effected conveniently.

B. Counting Equipment

1. Non-portable

The counting equipment used for the experimental data consisted of a decade scaler, Model 181A, manufactured by the Nuclear-Chicago Corporation.

The detector used was a Nuclear-Chicago scintillation detector, Model DS-1A. The detector was operated at a voltage of 1200 v. with the directional shield on.

2. Portable

Counting checks and preliminary mapping were done with a portable radiation meter, type 2610.

C. Source

A 100 millicurie radium-beryllium source was provided as the extraneous source for the assembly. For purposes of calculation it was regarded as a point source suspended 27 inches from the top of the assembly.

Figure 11. View of assembly showing location of lattice in spacer plate

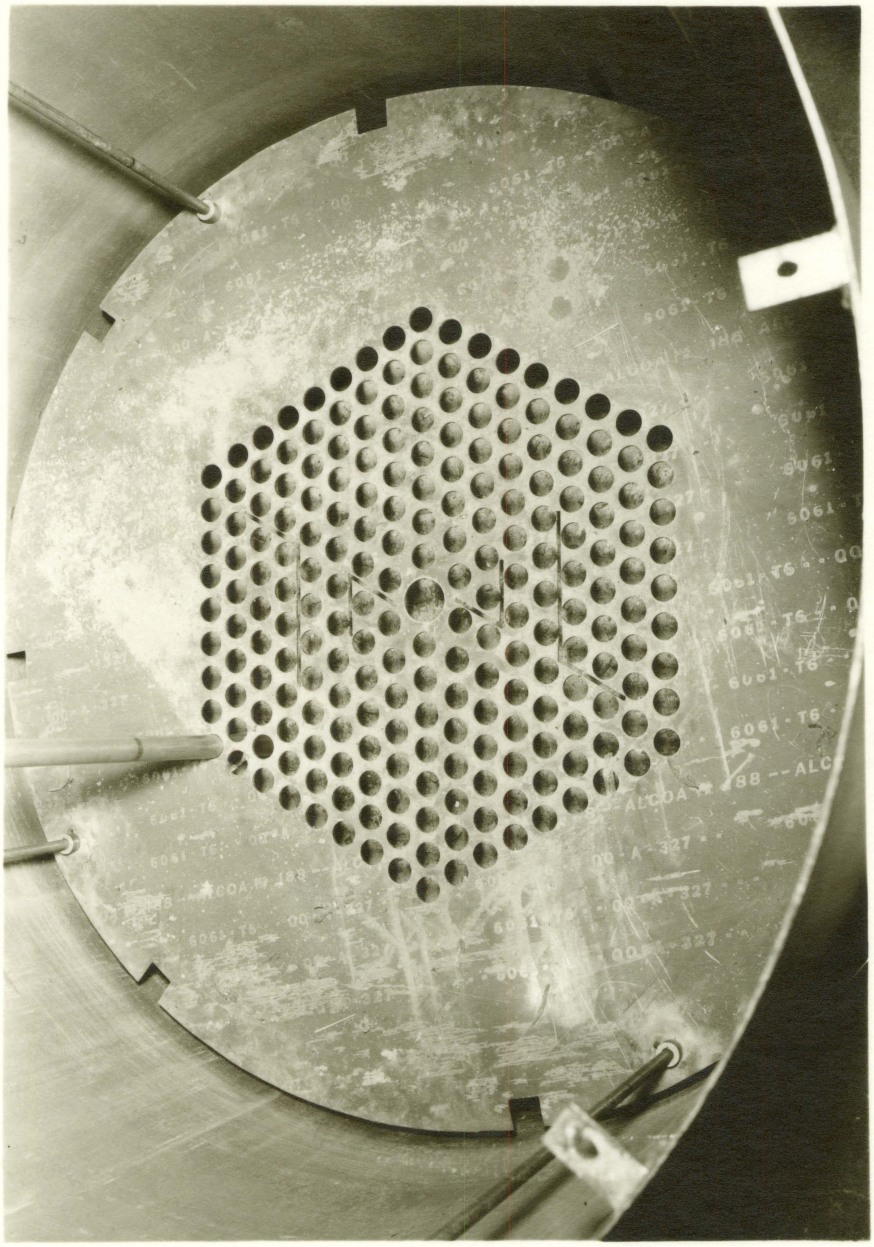

Figure 12. View of assembly with representation of fuel rod

VI. PROCEDURE

The counting procedure was a very simple one requiring no special techniques. The periphery of the shell in the horizontal plane of the source was marked every five degrees, and in the vicinity of the vertices of the lattice the interval of measurement was reduced to 2-1/2 degrees. Counts were then made at all marked locations. During the count, the midpoint of the detector was placed on the marked location and the projected area of the detector was used to calculate a "per centimeter" counting rate.

During the time the count was made, background counts were conducted intermittently; but since all counts were accomplished during one continuous session the background varied little.

The source was positioned in the assembly by means of a hollowed wooden cup that served as a container for the source. This cup was suspended in the source tube and because its diameter so nearly approximated that of the tube there was little room for movement; and the position of the source was therefore assured.

VII. RESULTS

The experimental results are listed in Appendix A and are depicted with the theoretical prediction in Figure 13. The solid line represents the experimental values obtained, whereas the dotted line represents calculated values. The correlation between the measured and calculated patterns of radiation is clearly evident. The measured values of the paths adjacent to the vertex path (path B), however, are greater than the values of the remaining non-vertex paths. This increase differs from the calculated pattern, for in the system of calculation employed, attenuation of the radiation to values below background was postulated for these paths. This difference between the theoretical and measured patterns of radiation indicates a scattering process near the vertex that results in a portion of the radiation of path A and path B escaping absorption and scattering into the point of measurement of path B.

The probable error listed in Appendix A was based upon the relationship

$$E = \frac{0.67\ (N)^{\frac{1}{2}}}{T}$$

where N represents the count measured and T the duration of the count.

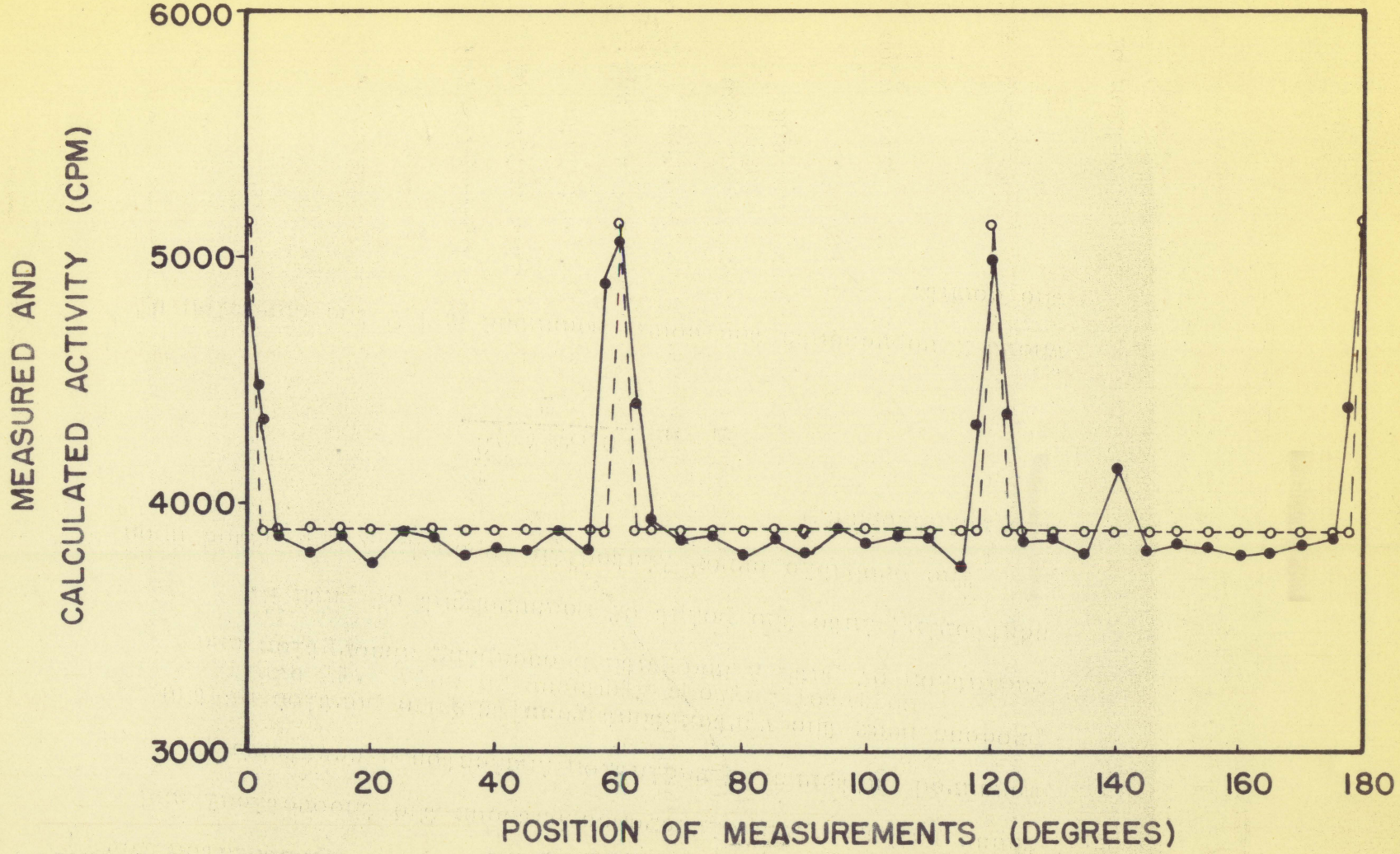

Figure 13a. Measured (——) and calculated (- - - -) radiation patterns

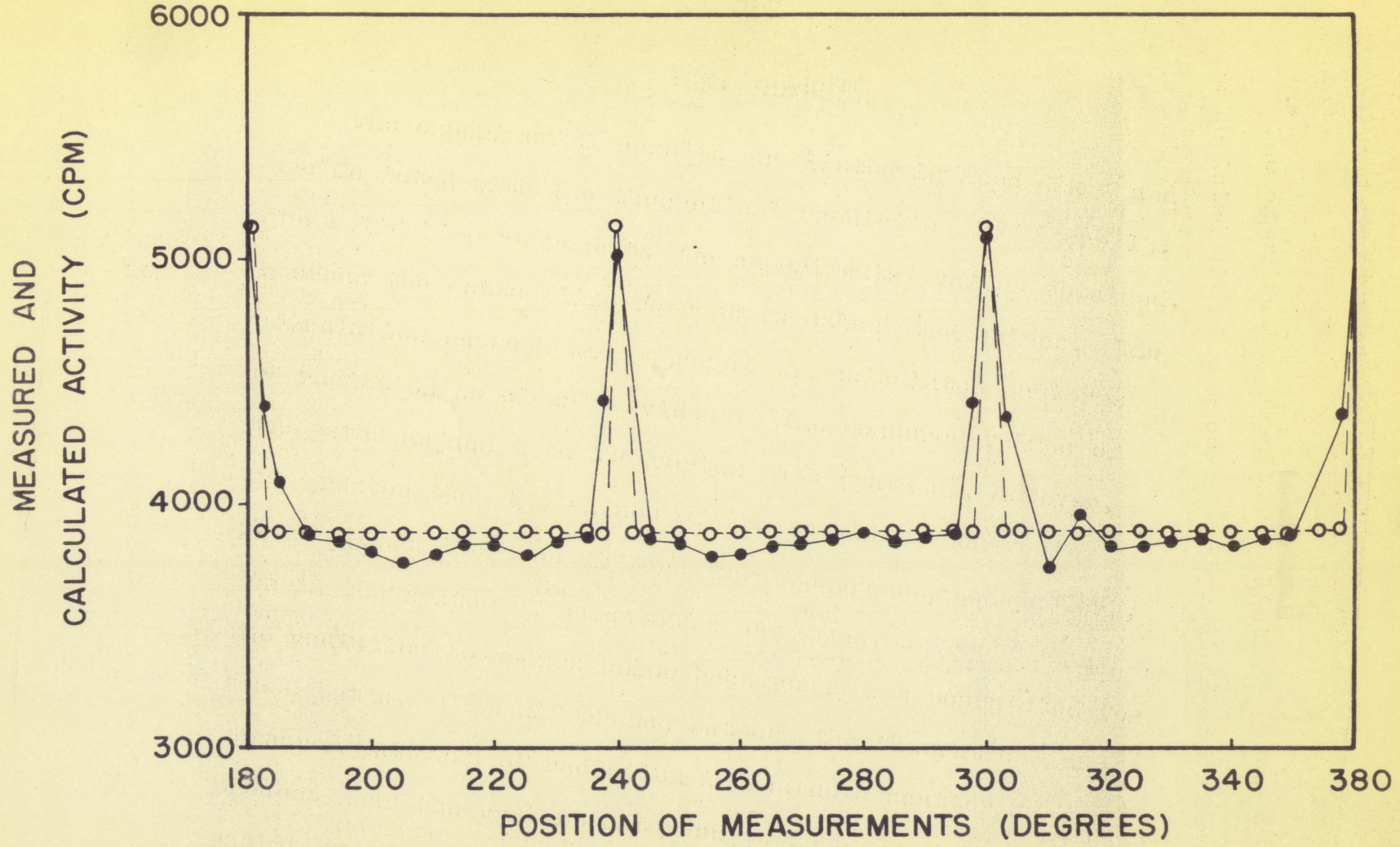

Figure 13b. Measured (——) and calculated (----) radiation patterns

VIII. DISCUSSION

The theoretical and measured patterns of radiation obtained from the previously-described systems of calculation and experiment show enough agreement to serve as an approximation of the true pattern. However, the exactness with which the patterns of this thesis reflect the true pattern is dependent upon the validity of the calculated approximations and the precision of the experimental method.

The approximations of major importance in the calculations will be discussed briefly. The decay pattern of the radium-beryllium source that was used in the calculations was one of many available. The weighting factors used in obtaining the groups of average energy also differ in the literature. The accuracy of the calculated radiation pattern is thus dependent on the reliability of the source from which the weighting factors were extracted.

The use of K_{∞} for K_{eff} tends to overestimate the neutron efficiency of the assembly and ultimately leads to high values of radiation.

The efficiency used for the detector was an average efficiency calculated for all the gamma rays counted by the detector. Since the greatest part of the issuing radiation results from the gamma-rays born in the lattice during fission, the detector must count gamma-rays in which a whole spectrum of various energies is present. The approximation

of this energy by Glasstone (7) is not precise, and the overall average energy used overweights the approximation in the direction of the source radiation.

In the absorption calculations the aluminum cladding was ignored. This probably represents an approximation that would introduce error in any solution wherein less than complete absorption is afforded by the lattice. In this calculation it is without effect, for its presence affects only the radiation paths through the lattice -- all radiation levels of which were reduced to values below background by the absorption of the water and uranium of the lattice. In the clear paths of the lattice discontinuities, where residual radiation exists, there is no aluminum. Without total absorption, however, this factor could not be ignored.

In the transformation from the volume source to the surface source (surface of the hexagonal lattice), the arithmetical average of flux was employed as an approximation for the whole lattice. This method tends to overestimate the strength of the equivalent surface source, since it gives equal weight to all parts of the volume-distributed source, whereas, most of the radiation reaching the surface arises from the outer regions of the volume where the source strength is less than in the interior. The presence of the water reflector tends to minimize this error, however.

Reciprocal scattering in a homogeneous medium was assumed in this thesis. This assumption would have applied to

the vertex paths through the wood cup and through the water reflector. By this assumption, the number of gamma-rays scattered out of the path through the cup would be equalled by the number scattered in. In this situation only the absorption coefficient would have been used in calculating the attenuation through the cup. Though the number of gamma-rays remains unchanged, the fact that their direction has been changed precludes their following the path of the vertex and causes them to enter the highly absorbing lattice. Since the scattered rays become absorbed, the total coefficient of attenuation is used to calculate the attenuation through the wood cup. In the water reflector, gamma-rays scattered out of the vertex path are not replaced by other rays being scattered in, for the radiation of the adjacent paths has already been absorbed by the lattice. Therefore, the total attenuation coefficient was again used. Consequently, though the assumption of reciprocal scattering was made, it did not enter into the calculations.

The attenuation calculations in all paths were always initially made with the highest energy radiation following those paths. When the radiation level at this energy was reduced to a value below background and the summation of this activity and the contributions of the lesser energies was determined to be also below background, the calculations were terminated. This was the case for calculations concerned with paths through the lattice. The summation of the radiation of

all energies following the vertex path, however, exceeded background; therefore the value of the summation was used in the attenuation calculations.

IX. CONCLUSIONS

As a result of this study, within the limits of this experiment, the following conclusions may be drawn:

1. Despite its density, when a hexagonal lattice is employed in an assembly of this type, the escape of gamma-radiation at the vertices of the lattice can be anticipated.

2. With regard to safety from gamma-radiation, consideration must be given these local areas of radiation in deciding upon the suitability of this design in satisfying the needs for a nuclear assembly.

3. Since the simplified system of analysis herein employed resulted in computed values of radiation that showed a definite correlation with the experimental values, this analytic solution may serve as a good first approximation of the expected radiation pattern of an assembly of this kind.

X. SELECTED REFERENCES

1. Bleuler, Ernst and Goldsmith, George J. Experimental nucleonics. New York, Rinehart & Company, Inc. 1952.

2. Davisson, Charlotte Meaker and Evans, Robley D. Measurements of gamma-ray absorption coefficients. Physical Review. 81: 404-411. 1951.

3. Foldy, L. L. Diffusion of high energy gamma-rays through matter. I. Fundamental equations. Physical Review. 81: 395-399. 1951.

4. Foldy, L. L. and Osborn, R. K. Diffusion of high energy gamma-rays through matter. II. Solution of the diffusion equations. Physical Review. 81: 400-404. 1951.

5. Friedlander, Gerhart and Kennedy, Joseph W. Nuclear and radiochemistry. 2nd ed. New York, John Wiley & Sons, Inc. 1955.

6. Glasstone, Samuel. Principles of nuclear reactor engineering. Princeton, N. J., D. Van Nostrand Company, Inc. 1955.

7. Glasstone, Samuel and Edlund, Milton C. Elements of nuclear reactor theory. New York, D. Van Nostrand Company, Inc. 1952.

8. Kaplan, Irving. Nuclear physics. Cambridge, Mass., Addison-Wesley Publishing Company, Inc. 1955.

9. Latter, Richard and Kahn, Herman. Gamma-ray absorption coefficients. Rand Corporation Report, R-170. 1949.

10. Murray, Raymond L. Introduction to nuclear engineering. Englewood Cliffs, N. J., Prentice-Hall, Inc. 1954.

11. Peebles, Glenn H. and Plesset, Milton S. Transmission of gamma-rays through large thicknesses of heavy materials. Physical Review. 81: 430-439. 1951.

12. Shapiro, Mathew M. Reactor statics; experimental and numerical results. In Reactor Handbook Vol. 1. pp. 477-530. U. S. Atomic Energy Commission Document No. 3645. [Washington], The Commission. Technical Information Service. Mar. 1955.

13. Snyder, W. S. and Powell, J. L. Absorption of γ-rays. U. S. Atomic Energy Commission Document No. 2739. Oak Ridge, Tenn., The Commission. Technical Information Division. 1949.

14. Uhrig, Robert E., Iowa State College, Ames, Iowa. Foil activation data. Private communication. 1956.

15. United States Atomic Energy Commission. New nuclear data, 1954 cumulation. Nuclear Science Abstracts. Vol. 8. No. 24B. Oak Ridge, Tenn. The Commission. Technical Information Service. Dec. 1954.

16. Webster, J. W. Practical reactor theory. U. S. Atomic Energy Commission Document No. 4083. Oak Ridge, Tenn., The Commission. Technical Information Extension. 1953.

17. Wolfe, William B. Gamma-ray scattering within thin-walled shells. Unpublished M. S. Thesis. Ames, Iowa, Iowa State College Library. 1957.

XI. APPENDICES

A. Appendix A

Table 4. Measured radiation pattern

Angle (degrees)	Efficiency (%)	Duration (minutes)	Background (cpm)	Reading (cpm)	Error (cpm)
0	33	3	125	4870	± 46
2.5				4330	± 44
5				3860	± 42
10				3800	± 41
15				3860	± 42
20				3760	± 41
25	33	3	125	3880	± 42
30				3860	± 42
35				3790	± 41
40				3820	± 41
45				3810	± 41
50	33	3	125	3880	± 42
55				3810	± 41
57.5				4880	± 46
60				5053	± 48
62.5				4400	± 44

Table 4. (Continued)

Angle (degrees)	Efficiency (%)	Duration (minutes)	Background (cpm)	Reading (cpm)	Error (cpm)
65	33	3	125	3930	± 42
70				3850	± 42
75				3870	± 42
80				3790	± 41
85				3860	± 42
90				3800	± 41
95				3900	± 42
100				3840	± 41
105				3870	± 42
110				3870	± 42
115				3750	± 41
117.5				4320	± 44
120				4920	± 47
122.5				4360	± 44
125				3850	± 42
130				3860	± 42
135				3800	± 41
140				4140	± 43
145				3820	± 41
150				3840	± 41

Table 4. (Continued)

Angle (degrees)	Efficiency (%)	Duration (minutes)	Background (cpm)	Reading (cpm)	Error (cpm)
155	33	3	125	3830	± 41
160				3800	± 41
165				3810	± 41
170				3840	± 41
175				3870	± 42
177.5				4400	± 44
180				5090	± 48
182.5				4390	± 44
185				4080	± 42
190				3860	± 42
195				3862	± 42
200				3810	± 41
205				3760	± 41
210				3800	± 41
215				3840	± 41
220				3841	± 41
225				3791	± 41
230				3850	± 42
235				3870	± 42

Table 4. (Continued)

Angle (degrees)	Efficiency (%)	Duration (minutes)	Background (cpm)	Reading (cpm)	Error (cpm)
237.5	33	3	125	4420	± 44
240				5007	± 47
242.5				4380	± 44
245				3860	± 42
250				3858	± 42
255				3790	± 41
260				3800	± 41
265				3832	± 41
270				3839	± 41
275				3861	± 42
280				3891	± 42
285				3852	± 42
290				3860	± 42
295				3874	± 42
297.5				4410	± 44
300				5090	± 48
302.5				4362	± 44
305				3890	± 42
310				3740	± 41
315				3950	± 42

Table 4. (Continued)

Angle (degrees)	Efficiency (%)	Duration (minutes)	Background (cpm)	Reading (cpm)	Error (cpm)
320	33	3	125	3824	± 41
325				3824	± 41
330				3859	± 42
335				3861	± 42
340				3821	± 41
345				3859	± 42
350				3861	± 42
355				3900	± 42
357.5				4371	± 44
360				4870	± 46

Table 5. Foil activation data

Position	Time	Duration (min)	Background (cpm)	Corrected activity (cpm)	Elapsed time (min)	$e^{-\lambda t}$	Equivalent activity (cpm)
1	0911	2	27.8	37	21	1.310	48
2	0914	2	27.8	48	24	1.361	65
3	0917	2	27.8	120	27	1.415	170
4	0920	2	27.8	217	30	1.470	319
5	0923	2	27.8	332	33	1.528	507
6	0925	2	27.8	569	35	1.568	892
7	0928	2	27.8	816	38	1.630	1332
8	0931	2	27.8	1304	41	1.694	2210
9	0934	2	27.8	2114	44	1.760	3732
10	0936	2	27.8	3235	46	1.860	5840
11	0939	2	27.8	3613	49	1.874	6760
12	0946	2	27.8	2325	56	2.052	4770

B. Appendix B

The average energies of the gamma-rays were calculated by the following formulae:

$$\text{Energy of first group } (E_1) = \frac{E_{11}W_{11} + E_{12}W_{12} + \text{etc}}{\Sigma (W_1)}$$

$$\text{Energy of second group } (E_2) = \frac{E_{21}W_{21} + E_{22}W_{22} + \text{etc}}{\Sigma (W_2)}$$

$$\text{Energy of third group } (E_3) = \frac{E_{31}W_{31} + E_{32}W_{32} + \text{etc}}{\Sigma (W_3)}$$

The weightings of the groups were made in the following manner:

$$F_1 = \frac{\Sigma (W_1)}{\Sigma (W_1) + \Sigma (W_2) + \Sigma (W_3)}$$

$$F_2 = \frac{\Sigma (W_2)}{\Sigma (W_1) + \Sigma (W_2) + \Sigma (W_3)}$$

$$F_3 = \frac{\Sigma (W_3)}{\Sigma (W_1) + \Sigma (W_2) + \Sigma (W_3)}$$

where E_1 = average energy of first group

E_{11} = energy of first gamma-ray of first group

W_{11} = weighting of first gamma-ray of first group

E_{12} = energy of second gamma-ray of first group

W_{12} = weighting of second gamma-ray of first group

E_2 = average energy of second group

E_{21} = energy of first gamma-ray of second group

E_{22} = energy of second gamma-ray of second group

W_{21} = weighting of first gamma-ray of second group

W_{22} = weighting of second gamma-ray of second group

E_3 = average energy of third group

E_{31} = energy of first gamma-ray of third group

E_{32} = energy of second gamma-ray of third group

W_{31} = weighting of first gamma-ray of third group

W_{32} = weighting of second gamma-ray of third group

$\Sigma(W_1)$ = summation of weighting of first group

$\Sigma(W_2)$ = summation of weightings of second group

$\Sigma(W_3)$ = summation of weightings of third group

F_1 = weighting factor of first group

F_2 = weighting factor of second group

F_3 = weighting factor of third group